ARMY RESEARCH LABORATORY

Developments In The Explicit Derivation of Hybrid Stress Finite Element Matrices

Erik Saether

ARL-TR-688

March 1995

The findings in this report are not to be construed as an official Department of the Army position unless so designated by other authorized documents.

Citation of manufacturer's or trade names does not constitute an official endorsement or approval of the use thereof.

Destroy this report when it is no longer needed. Do not return it to the originator.

REPORT DOCUMENTATION PAGE

Form Approved
OMB No. 0704-0188

1. AGENCY USE ONLY *(Leave blank)*	2. REPORT DATE	3. REPORT TYPE AND DATES COVERED
	March 1995	Final 1/95 - 3/95

4. TITLE AND SUBTITLE
Developments in the Explicit Derivation of Hybrid Stress Finite Element Matrices

5. FUNDING NUMBERS

6. AUTHOR(S)
Erik Saether

7. PERFORMING ORGANIZATION NAME(S) AND ADDRESS(ES)
Army Research Laboratory
Watertown, MA 02172-0001
ATTN: AMSRL-MA-PC

8. PERFORMING ORGANIZATION REPORT NUMBER
ARL-TR-688

9. SPONSORING/MONITORING AGENCY NAME(S) AND ADDRESS(ES)

10. SPONSORING/MONITORING AGENCY REPORT NUMBER

11. SUPPLEMENTARY NOTES

12a. DISTRIBUTION/AVAILABILITY STATEMENT
Approved for public release; distribution unlimited.

12b. DISTRIBUTION CODE

13. ABSTRACT *(Maximum 200 words)*

A general methodology for deriving explicit element stiffness matrices in hybrid stress formulations has recently been developed by the author. The technique utilizes special stress field transformations to eliminate the complementary energy matrix inherent to hybrid formulations thus simplifying the constituent matrices such that an explicit evaluation can be accomplished. The elimination of numerical integration and matrix inversions result in a substantial decrease in computational cost. The methodology is demonstrated by deriving explicit algebraic expressions for the Pian-Tong hexahedral element stiffness matrix and in the development of an explicit form of the Pian-Sumihara quadrilateral element incorporating nonconstant material properties for nonlinear–elastic analyses.

14. SUBJECT TERMS	15. NUMBER OF PAGES
Finite Element Theory, Hybrid Stress Method	24
	16. PRICE CODE

17. SECURITY CLASSIFICATION OF REPORT	18. SECURITY CLASSIFICATION OF THIS PAGE	19. SECURITY CLASSIFICATION OF ABSTRACT	20. LIMITATION OF ABSTRACT
Unclassified	Unclassified	Unclassified	UL

Contents

Figures

Tables

Appendices

INTRODUCTION

Continuing research into hybrid stress finite element formulations has been directed towards minimizing the computational cost associated with computing element stiffness coefficients in order to make hybrid elements competitive with purely displacement–based formulations. Much emphasis has been placed on reducing the computational cost of inverting the complementary energy or flexibility matrix inherent to the hybrid stress method and has led to insightful yet elaborate procedures and approximations directed towards this aim[1,2,3]. Recently, a general procedure has been developed by the author for simplifying the stiffness definition by making full use of the freedom in selecting and manipulating assumed stress fields which include the generation of a weighted orthonormalized stress mode basis[4]. In this approach, the flexibility matrix is formally eliminated and the resulting expression for the element stiffness matrix is reduced to the integration of a single constituent matrix which can be accomplished in closed–form. Such an evaluation results in algebraic equations which can appear cumbersome; however, these statements replace the formation and inversion of the flexibility matrix and, more importantly, the costly numerical quadrature of large–order matrix products. In contrast, displacement–based continuum elements under general distortion possess an integrand involving rational functions due to the presence of the Jacobian determinant in the denominator which precludes a simple explicit evaluation of stiffness coefficients in algebraic form. Such a represention of basic strain energy characteristics by rational functions compounded by possible nonlinear variations in material properties make the inherent polynomial approximation of Gaussian quadrature schemes significant in regards to the rate of solution convergence. The present method is completely generic and potentially avoids all approximations made to the formal variational definition of hybrid element stiffness matrices. The developed technique is utilized in two different element derivations. First, a closed-form set of expressions are developed for the stiffness coefficients in the Pian-Tong hexahedral element[5] which is a robust 8-node solid continuum element and presents a formidable degree of difficulty in deriving an explicit formulation. Secondly, the method is extended to derive explicit expressions for element stiffness matrices incorporating nonconstant material properties for nonlinear–elastic problems which, within the framework of finite element solution methods, usually require computationally intensive, iterative solution procedures. As an initial effort towards that aim, an explicit formulation is developed for the 4–node Pian-Sumihara hybrid quadrilateral element[6]. The resulting closed-form derivations demonstrate a substantial reduction in computational cost over purely numerical treatments in generating element matrices.

VARIATIONAL BASIS OF THE HYBRID MODEL

The form of the Hellinger-Reissner energy functional utilized in References [5] and [6] is given by

$$\Pi_R = \int_v [(-1/2)\boldsymbol{\sigma}^T \mathbf{S}\boldsymbol{\sigma} + \boldsymbol{\sigma}^T(\mathbf{L}\mathbf{u}_q) - (\mathbf{L}^T\boldsymbol{\sigma})^T\mathbf{u}_\lambda]dv \tag{1}$$

where $\boldsymbol{\sigma}$ is the assumed stress field, $\mathbf{S}$ is the material compliance matrix, $\mathbf{u}_q$ and $\mathbf{u}_\lambda$ are the assumed compatible and incompatible displacement fields and $\mathbf{L}$ is the differential operator relating strains to displacements. The assumed stresses may be represented by

$$\boldsymbol{\sigma} = \boldsymbol{P}\boldsymbol{\beta} \tag{2}$$

where $\mathbf{P}$ is a matrix of polynomial terms and $\boldsymbol{\beta}$ is a vector of undetermined expansion coefficients. The displacement field is assumed over the element domain as

$$\mathbf{u} = \mathbf{u}_q + \mathbf{u}_\lambda = \mathbf{N}\mathbf{q} + \mathbf{M}\boldsymbol{\lambda} \tag{3}$$

where $\mathbf{N}$ and $\mathbf{M}$ are compatible and incompatible displacement shape functions, respectively, $\mathbf{q}$ are nodal displacements, and $\boldsymbol{\lambda}$ are Lagrange multipliers which variationally enforce the field equilibrium conditions. These variational constraints are applied *a priori* to the assumed stress modes which condense the influence of the incompatible modes into the element formulation. The resulting expression for the element stiffness matrix is given by

$$\mathbf{K} = \mathbf{G}^T\mathbf{H}^{-1}\mathbf{G} \tag{4}$$

where

$$\mathbf{H} = \int_v \mathbf{P}^T\mathbf{S}\mathbf{P}dv \tag{5}$$

$$\mathbf{G} = \int_v \mathbf{P}^T \mathbf{B} dv \tag{6}$$

in which $\mathbf{B}$ is the strain-displacement matrix. In the above formulation, the *a priori* condensation of the incompatible displacement modes results in an $\mathbf{H}$ matrix which is fully populated and has hitherto required the inversion of a full matrix of order $dim(\beta)$.

COMPUTATION OF EXPLICIT STIFFNESS MATRICES

The procedure developed in Reference [4] for simplifying the expressions involved in (4) is outlined below. The method utilizes a sequence of permissible transformations of assumed stress fields to simplify the stiffness definition. The assumed stresses are first transformed through the introduction of a symmetric 'distributing' matrix as

$$\mathbf{P} = \mathbf{IP} = (\mathbf{DD}^{-1})\mathbf{P} = \mathbf{D}(\mathbf{D}^{-1}\mathbf{P}) = \mathbf{D}\bar{\mathbf{P}} \tag{7}$$

where the distributing matrix is defined as

$$\mathbf{D} = \mathbf{S}^{-1/2} \tag{8}$$

The inverse square root of the compliance matrix is obtained through a standard spectral decomposition[7]. For illustration, the decomposition of 2–D and 3–D orthotropic compliance matrices are presented in Appendix I. Substitution of (7) into (5) yields

$$\mathbf{H} = \int_{-1}^{1}\int_{-1}^{1}\int_{-1}^{1} [|\mathbf{J}|\bar{\mathbf{P}}^T \mathbf{D}^T \mathbf{S}\mathbf{D}\bar{\mathbf{P}}] d\xi d\eta d\zeta \tag{9}$$

where, from the definition of $\mathbf{D}$ and the symmetry of both $\mathbf{S}$ and $\mathbf{D}$, we obtain

$$\mathbf{D}^T\mathbf{S}\mathbf{D} = \mathbf{S}^{-1/2}\mathbf{S}\mathbf{S}^{-1/2} = \mathbf{S}\mathbf{S}^{-1} = \mathbf{I}$$

and the flexibility matrix reduces to

$$\mathbf{H} = \int_{-1}^{1}\int_{-1}^{1}\int_{-1}^{1} [|\mathbf{J}|\bar{\mathbf{P}}^T \bar{\mathbf{P}}] d\xi d\eta d\zeta \tag{10}$$

A second field transformation uses equation (10) to define a weighted inner product for use in a Gram-Schmidt procedure to generate an orthonormal spanning set of stress modes, $\mathbf{P}^*$, which are a special linear combination of the modes present in $\bar{\mathbf{P}}$. The weighted inner product is therefore defined as

$$< \bar{\mathbf{P}}_i, \bar{\mathbf{P}}_j > = \int_{-1}^{1}\int_{-1}^{1}\int_{-1}^{1} [|\mathbf{J}|\bar{\mathbf{P}}_i^T \bar{\mathbf{P}}_j] d\xi d\eta d\zeta = \delta_{ij} \tag{11}$$

where δ_{ij} is the Kronecker delta function. The linear combination yielding a sequence of orthogonal stress modes is given by

$$\mathbf{V}_i = \begin{cases} \bar{\mathbf{P}}_i & i = 1 \\ \bar{\mathbf{P}}_i - \sum_{j=1}^{i-1} < \mathbf{P}_j^*, \bar{\mathbf{P}}_i > \mathbf{P}_j^* & i > 1 \end{cases} \tag{12}$$

which are normalized to form basis vectors, $\mathbf{P}_i^*$, as

$$\mathbf{P}_i^* = < \mathbf{V}_i, \mathbf{V}_i >^{-1/2} \mathbf{V}_i \tag{13}$$

Substitution of $\mathbf{P}^*$ into equation (10) yields by definition

$$\mathbf{H} = \int_{-1}^{1}\int_{-1}^{1}\int_{-1}^{1} [|\mathbf{J}|\mathbf{P}^{*T}\mathbf{P}^*] d\xi d\eta d\zeta \equiv \mathbf{I} \tag{14}$$

The new basis for the element stress field is now given by

$$\mathbf{P} = \mathbf{D}\mathbf{P}^* \tag{15}$$

and the expression for the element stiffness matrix reduces to

$$\mathbf{K} = \mathbf{G}^T\mathbf{G} \tag{16}$$

Separating out the Jacobian determinant from the isoparametric strains as

$$\mathbf{B} = \frac{1}{|\mathbf{J}|}\mathbf{B}^*(\xi,\eta,\zeta) \tag{17}$$

and substituting (15) and (17) into (6) yields the **G** matrix definition as

$$\mathbf{G} = \int_{-1}^{1}\int_{-1}^{1}\int_{-1}^{1}[\mathbf{P}^{*T}\mathbf{D}\mathbf{B}^*]d\xi d\eta d\zeta \tag{18}$$

The absence of the Jacobian determinant in the denominator permits a direct derivation of algebraic expressions for the **G** matrix coefficients. The explicit form of the element stiffness matrix is then obtained from equation (16).

EXPLICIT PIAN-TONG HEXAHEDRAL ELEMENT

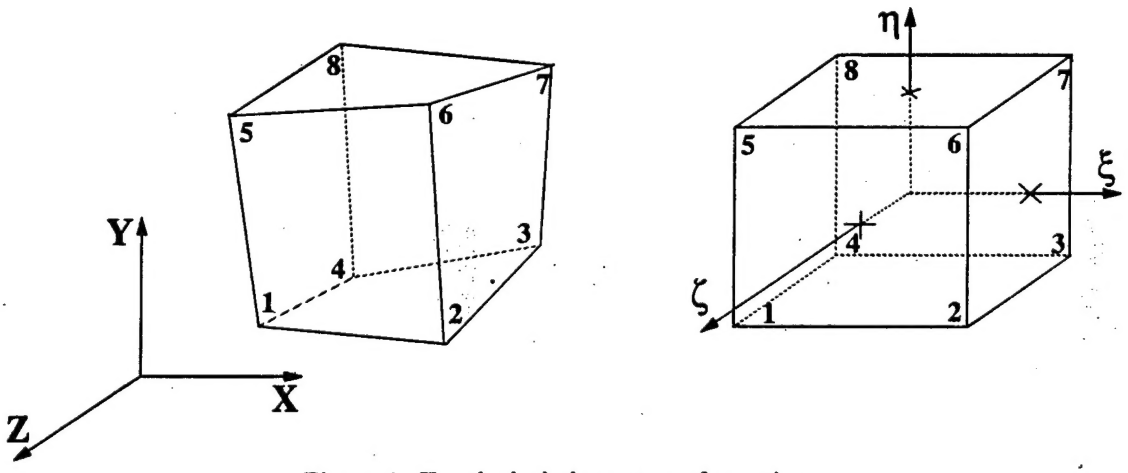

Figure 1. Hexahedral element configuration.

The configuration of the 8-node Pian-Tong hexahedral element is depicted in Figure 1. The compatible displacement functions $\mathbf{u}_q$ are given by

$$\mathbf{u}_q = \begin{Bmatrix} u_q \\ v_q \\ w_q \end{Bmatrix} = \sum_{i=1}^{8}\frac{1}{8}(1+\xi_i\xi)(1+\eta_i\eta)(1+\zeta_i\zeta)\begin{Bmatrix} u_i \\ v_i \\ w_i \end{Bmatrix} \tag{19}$$

As detailed in Reference [5], incompatible displacement modes are introduced to complete the cubic order of the assumed isoparametric displacement field. These modes are condensed *a priori* into the element formulation through constraint conditions on the assumed stress modes.

The stress field utilized in the Pian-Tong element is assumed in natural coordinates and transformed to physical coordinates using Jacobians computed at the element centroid as

$$\sigma^{kl} = (J_o)_i^k(J_o)_j^l\tau^{ij} \tag{20}$$

Performing the initial transformation of stresses given by (7) results in the physical or Cartesian stress field given by

$$\boldsymbol{\sigma} = [\sigma_x,\sigma_y,\sigma_z,\tau_{yz},\tau_{zx},\tau_{xy}]^T = \bar{\mathbf{P}}_c\boldsymbol{\beta}_c + \bar{\mathbf{P}}_h\boldsymbol{\beta}_h \tag{21}$$

where

$$\bar{\mathbf{P}}_c = \begin{bmatrix} 1 & & & & & & \\ & 1 & & & & & \\ & & 1 & & & & \\ & & & 1 & & & \\ & & & & 1 & & \\ & & & & & 1 & \end{bmatrix} \tag{22}$$

and

$$\bar{\mathbf{P}}_h = \begin{bmatrix} e_{12}\xi & e_{13}\xi & e_{15}\xi & e_{11}\eta & e_{13}\eta & e_{16}\eta & e_{11}\zeta & e_{12}\zeta & e_{14}\zeta & e_{13}\xi\eta & e_{11}\eta\zeta & e_{12}\xi\zeta \\ e_{22}\xi & e_{23}\xi & e_{25}\xi & e_{21}\eta & e_{23}\eta & e_{26}\eta & e_{21}\zeta & e_{22}\zeta & e_{24}\zeta & e_{23}\xi\eta & e_{21}\eta\zeta & e_{22}\xi\zeta \\ e_{32}\xi & e_{33}\xi & e_{35}\xi & e_{31}\eta & e_{33}\eta & e_{36}\eta & e_{31}\zeta & e_{32}\zeta & e_{34}\zeta & e_{33}\xi\eta & e_{31}\eta\zeta & e_{32}\xi\zeta \\ e_{42}\xi & e_{43}\xi & e_{45}\xi & e_{41}\eta & e_{43}\eta & e_{46}\eta & e_{41}\zeta & e_{42}\zeta & e_{44}\zeta & e_{43}\xi\eta & e_{41}\eta\zeta & e_{42}\xi\zeta \\ e_{52}\xi & e_{53}\xi & e_{55}\xi & e_{51}\eta & e_{53}\eta & e_{56}\eta & e_{51}\zeta & e_{52}\zeta & e_{54}\zeta & e_{53}\xi\eta & e_{51}\eta\zeta & e_{52}\xi\zeta \\ e_{62}\xi & e_{63}\xi & e_{65}\xi & e_{61}\eta & e_{63}\eta & e_{66}\eta & e_{61}\zeta & e_{62}\zeta & e_{64}\zeta & e_{63}\xi\eta & e_{61}\eta\zeta & e_{62}\xi\zeta \end{bmatrix} \tag{23}$$

The coefficients e_{ij} are obtained from the product of the inverse distributing matrix and a transformation matrix relating tensorial stresses to physical components. This relationship is given by

$$\mathbf{E} = \mathbf{D}^{-1}\mathbf{T}$$

or

$$[e_{ij}] = \begin{bmatrix} \bar{d}_{11} & \bar{d}_{12} & \bar{d}_{13} & & & \\ \bar{d}_{21} & \bar{d}_{22} & \bar{d}_{23} & & & \\ \bar{d}_{31} & \bar{d}_{32} & \bar{d}_{33} & & & \\ & & & \bar{d}_{44} & & \\ & & & & \bar{d}_{55} & \\ & & & & & \bar{d}_{66} \end{bmatrix} \begin{bmatrix} a_1^2 & a_2^2 & a_3^2 & 2a_1a_2 & 2a_2a_3 & 2a_1a_3 \\ b_1^2 & b_2^2 & b_3^2 & 2b_1b_2 & 2b_2b_3 & 2b_1b_3 \\ c_1^2 & c_2^2 & c_3^2 & 2c_1c_2 & 2c_2c_3 & 2c_1c_3 \\ a_1c_1 & a_2c_2 & a_3c_3 & a_2c_1 + a_1c_2 & a_3c_2 + a_2c_3 & a_3c_1 + a_1c_3 \\ a_1b_1 & a_2b_2 & a_3b_3 & a_1b_2 + a_2b_1 & a_2b_3 + a_3b_2 & a_1b_3 + a_3b_1 \\ b_1c_1 & b_2c_2 & b_3c_3 & b_1c_2 + b_2c_1 & b_2c_3 + b_3c_2 & b_1c_3 + b_3c_1 \end{bmatrix}$$

The isoparametric mapping between local physical and natural coordinates is given by

$$\begin{aligned} x &= a_1\xi + a_2\eta + a_3\zeta + a_4\xi\eta + a_5\xi\zeta + a_6\eta\zeta + a_7\xi\eta\zeta \\ y &= b_1\xi + b_2\eta + b_3\zeta + b_4\xi\eta + b_5\xi\zeta + b_6\eta\zeta + b_7\xi\eta\zeta \\ z &= c_1\xi + c_2\eta + c_3\zeta + c_4\xi\eta + c_5\xi\zeta + c_6\eta\zeta + c_7\xi\eta\zeta \end{aligned} \tag{24}$$

where

$$\begin{bmatrix} a_1 & b_1 & c_1 \\ a_2 & b_2 & c_2 \\ a_3 & b_3 & c_3 \\ a_4 & b_4 & c_4 \\ a_5 & b_5 & c_5 \\ a_6 & b_6 & c_6 \\ a_7 & b_7 & c_7 \end{bmatrix} = \frac{1}{8} \begin{bmatrix} -1 & 1 & 1 & -1 & -1 & 1 & 1 & -1 \\ -1 & -1 & -1 & -1 & 1 & 1 & 1 & 1 \\ 1 & 1 & -1 & -1 & 1 & 1 & -1 & -1 \\ 1 & -1 & -1 & 1 & -1 & 1 & 1 & -1 \\ -1 & 1 & -1 & 1 & -1 & 1 & -1 & 1 \\ -1 & -1 & 1 & 1 & 1 & 1 & -1 & -1 \\ 1 & -1 & 1 & -1 & -1 & 1 & -1 & 1 \end{bmatrix} \begin{bmatrix} x_1 & y_1 & z_1 \\ x_2 & y_2 & z_2 \\ x_3 & y_3 & z_3 \\ x_4 & y_4 & z_4 \\ x_5 & y_5 & z_5 \\ x_6 & y_6 & z_6 \\ x_7 & y_7 & z_7 \\ x_8 & y_8 & z_8 \end{bmatrix}$$

Orthonormalizing the stress modes according to (12) yields the final transformed stress field composed of constant modes given by

$$\mathbf{P}_c^* = n_1\bar{\mathbf{P}}_c \tag{25}$$

and higher–order modes given by

$$\mathbf{P}_h^* = [p_7^*, p_8^*, p_9^*, p_{10}^*, p_{11}^*, p_{12}^*, p_{13}^*, p_{14}^*, p_{15}^*, p_{16}^*, p_{17}^*, p_{18}^*] \tag{26}$$

The columns of the higher–order stress modes with $i = 1, 2, 3, ..., 6$ and $j = 1, 2, 3$ are given by

$$
\begin{aligned}
\{p^*_{i,j+6}\} &= n_{j+6}\{r_{i,2j-1}\xi + r_{i,2j}\} \\
\{p^*_{i,j+9}\} &= n_{j+9}\{r_{i,3j+4}\eta + r_{i,3j+5}\xi + r_{i,3j+6}\} \\
\{p^*_{i,j+12}\} &= n_{j+12}\{r_{i,4j+12}\zeta + r_{i,4j+13}\eta + r_{i,4j+14}\xi + r_{i,4j+15}\} \\
\{p^*_{i,16}\} &= n_{16}\{r_{i,28}\xi\eta + r_{i,29}\zeta + r_{i,30}\eta + r_{i,31}\xi + r_{i,32}\} \\
\{p^*_{i,17}\} &= n_{17}\{r_{i,33}\eta\zeta + r_{i,34}\xi\eta + r_{i,35}\zeta + r_{i,36}\eta + r_{i,37}\xi + r_{i,38}\} \\
\{p^*_{i,18}\} &= n_{18}\{r_{i,39}\xi\zeta + r_{i,40}\eta\zeta + r_{i,41}\xi\eta + r_{i,42}\zeta + r_{i,43}\eta + r_{i,44}\xi + r_{i,45}\}
\end{aligned}
$$

where the expressions for n_i and $r_{i,j}$ are presented in Appendix II.

The integration of (18) yields the following expressions for elements of the **G** matrix in which $j = 1, 2, 3, ..., 8$. Specific components utilize an additional index, i, which assumes the values $i = 1, 2, 3$. The components are given by

$$
\begin{aligned}
g_{i,3j-2} &= d_{1i}\Gamma_1(1,j) & g_{i,3j-1} &= d_{2i}\Gamma_1(2,j) & g_{i,3j} &= d_{3i}\Gamma_1(3,j) \\
g_{4,3j-2} &= 0 & g_{4,3j-1} &= d_{44}\Gamma_1(3,j) & g_{4,3j} &= d_{44}\Gamma_1(2,j) \\
g_{5,3j-2} &= d_{55}\Gamma_1(3,j) & g_{5,3j-1} &= 0 & g_{5,3j} &= d_{55}\Gamma_1(1,j) \\
g_{6,3j-2} &= d_{66}\Gamma_1(2,j) & g_{6,3j-1} &= d_{66}\Gamma_1(1,j) & g_{6,3j} &= 0
\end{aligned}
$$

$$
\begin{aligned}
g_{i+6,3j-2} &= d_{11}\Gamma_2(1,4,i,j) + d_{12}\Gamma_2(2,4,i,j) + d_{13}\Gamma_2(3,4,i,j) + d_{55}\Gamma_2(5,6,i,j) + d_{66}\Gamma_2(6,5,i,j) \\
g_{i+6,3j-1} &= d_{21}\Gamma_2(1,5,i,j) + d_{22}\Gamma_2(2,5,i,j) + d_{23}\Gamma_2(3,5,i,j) + d_{44}\Gamma_2(4,6,i,j) + d_{66}\Gamma_2(6,4,i,j) \\
g_{i+6,3j} &= d_{31}\Gamma_2(1,6,i,j) + d_{32}\Gamma_2(2,6,i,j) + d_{33}\Gamma_2(3,6,i,j) + d_{44}\Gamma_2(4,5,i,j) + d_{55}\Gamma_2(5,4,i,j) \\
g_{i+9,3j-2} &= d_{11}\Gamma_3(1,7,i,j) + d_{12}\Gamma_3(2,7,i,j) + d_{13}\Gamma_3(3,7,i,j) + d_{55}\Gamma_3(5,9,i,j) + d_{66}\Gamma_3(6,8,i,j) \quad (27) \\
g_{i+9,3j-1} &= d_{21}\Gamma_3(1,8,i,j) + d_{22}\Gamma_3(2,8,i,j) + d_{23}\Gamma_3(3,8,i,j) + d_{44}\Gamma_3(4,9,i,j) + d_{66}\Gamma_3(6,7,i,j) \\
g_{i+9,3j} &= d_{31}\Gamma_3(1,9,i,j) + d_{32}\Gamma_3(2,9,i,j) + d_{33}\Gamma_3(3,9,i,j) + d_{44}\Gamma_3(4,8,i,j) + d_{55}\Gamma_3(5,7,i,j) \\
g_{i+12,3j-2} &= d_{11}\Gamma_4(1,10,i,j) + d_{12}\Gamma_4(2,10,i,j) + d_{13}\Gamma_4(3,10,i,j) + d_{55}\Gamma_4(5,12,i,j) + d_{66}\Gamma_4(6,11,i,j) \\
g_{i+12,3j-1} &= d_{21}\Gamma_4(1,11,i,j) + d_{22}\Gamma_4(2,11,i,j) + d_{23}\Gamma_4(3,11,i,j) + d_{44}\Gamma_4(4,12,i,j) + d_{66}\Gamma_4(6,10,i,j) \\
g_{i+12,3j} &= d_{31}\Gamma_4(1,12,i,j) + d_{32}\Gamma_4(2,12,i,j) + d_{33}\Gamma_4(3,12,i,j) + d_{44}\Gamma_4(4,11,i,j) + d_{55}\Gamma_4(5,10,i,j) \\
g_{16,3j-2} &= d_{11}\Gamma_5(1,13,j) + d_{12}\Gamma_5(2,13,j) + d_{13}\Gamma_5(3,13,j) + d_{55}\Gamma_5(5,15,j) + d_{66}\Gamma_5(6,14,j) \\
g_{16,3j-1} &= d_{21}\Gamma_5(1,14,j) + d_{22}\Gamma_5(2,14,j) + d_{23}\Gamma_5(3,14,j) + d_{44}\Gamma_5(4,15,j) + d_{66}\Gamma_5(6,13,j) \\
g_{16,3j} &= d_{31}\Gamma_5(1,15,j) + d_{32}\Gamma_5(2,15,j) + d_{33}\Gamma_5(3,15,j) + d_{44}\Gamma_5(4,14,j) + d_{55}\Gamma_5(5,13,j) \\
g_{17,3j-2} &= d_{11}\Gamma_6(1,16,j) + d_{12}\Gamma_6(2,16,j) + d_{13}\Gamma_6(3,16,j) + d_{55}\Gamma_6(5,18,j) + d_{66}\Gamma_6(6,17,j) \\
g_{17,3j-1} &= d_{21}\Gamma_6(1,17,j) + d_{22}\Gamma_6(2,17,j) + d_{23}\Gamma_6(3,17,j) + d_{44}\Gamma_6(4,18,j) + d_{66}\Gamma_6(6,16,j) \\
g_{17,3j} &= d_{31}\Gamma_6(1,18,j) + d_{32}\Gamma_6(2,18,j) + d_{33}\Gamma_6(3,18,j) + d_{44}\Gamma_6(4,17,j) + d_{55}\Gamma_6(5,16,j) \\
g_{18,3j-2} &= d_{11}\Gamma_7(1,19,j) + d_{12}\Gamma_7(2,19,j) + d_{13}\Gamma_7(3,19,j) + d_{55}\Gamma_7(5,21,j) + d_{66}\Gamma_7(6,20,j) \\
g_{18,3j-1} &= d_{21}\Gamma_7(1,20,j) + d_{22}\Gamma_7(2,20,j) + d_{23}\Gamma_7(3,20,j) + d_{44}\Gamma_7(4,21,j) + d_{66}\Gamma_7(6,19,j) \\
g_{18,3j} &= d_{31}\Gamma_7(1,21,j) + d_{32}\Gamma_7(2,21,j) + d_{33}\Gamma_7(3,21,j) + d_{44}\Gamma_7(4,20,j) + d_{55}\Gamma_7(5,19,j)
\end{aligned}
$$

where d_{ij} are elements of the distributing matrix and the functions Γ_i are given by

$$
\begin{aligned}
\Gamma_1(m,j) &= n_1\phi_{j,m}/3 \\
\Gamma_2(k,m,i,j) &= n_{i+6}(r_{k,2i-1}\phi_{j,m} + r_{k,2i}\phi_{j,m-3})/9 \\
\Gamma_3(k,m,i,j) &= n_{i+9}(r_{k,3i+4}\phi_{j,m} + r_{k,3i+5}\phi_{j,m-3} + r_{k,3i+6}\phi_{j,m-6})/9 \\
\Gamma_4(k,m,i,j) &= n_{i+12}(r_{k,4i+12}\phi_{j,m} + r_{k,4i+13}\phi_{j,m-3} + r_{k,4i+14}\phi_{j,m-6} + r_{k,4i+15}\phi_{j,m-9})/9 \\
\Gamma_5(k,m,j) &= n_{16}(r_{k,28}\phi_{j,m} + r_{k,29}\phi_{j,m-3} + r_{k,30}\phi_{j,m-6} + r_{k,31}\phi_{j,m-9} + r_{k,32}\phi_{j,m-12})/27 \\
\Gamma_6(k,m,j) &= n_{17}(r_{k,33}\phi_{j,m} + r_{k,34}\phi_{j,m-3} + r_{k,35}\phi_{j,m-6} + r_{k,36}\phi_{j,m-9} + r_{k,37}\phi_{j,m-12} + r_{k,38}\phi_{j,m-15})/27 \\
\Gamma_7(k,m,j) &= n_{18}(r_{k,39}\phi_{j,m} + r_{k,40}\phi_{j,m-3} + r_{k,41}\phi_{j,m-6} + r_{k,42}\phi_{j,m-9} + r_{k,43}\phi_{j,m-12} + \\
&\qquad r_{k,44}\phi_{j,m-15} + r_{k,45}\phi_{j,m-18})/27
\end{aligned}
$$

The functions $\phi_{j,i}$, for $i = 1, 2, 3$, are given by

$$\begin{aligned}
\phi_{j,i} &= (\delta^i_{56} + 3\delta^i_{12})z^j_7 + (\delta^i_{35} + \delta^i_{42})z^j_6 + (\delta^i_{64} + 3\delta^i_{31})z^j_5 + (\delta^i_{63} + \delta^i_{14})z^j_3 + (\delta^i_{26} + \delta^i_{51})z^j_2 + (\delta^i_{45} + 3\delta^i_{23})z^j_1 \\
\phi_{j,i+3} &= (\delta^i_{57} + 3\delta^i_{14})z^j_7 + (\delta^i_{74} + 3\delta^i_{51})z^j_5 + (\delta^i_{35} + \delta^i_{42})z^j_4 + (\delta^i_{73} + 3\delta^i_{12})z^j_3 + (\delta^i_{27} + 3\delta^i_{31})z^j_2 + 3(\delta^i_{25} + \delta^i_{43})z^j_1 \\
\phi_{j,i+6} &= (\delta^i_{76} + 3\delta^i_{42})z^j_7 + (\delta^i_{37} + 3\delta^i_{12})z^j_6 + 3(\delta^i_{61} + \delta^i_{34})z^j_5 + (\delta^i_{63} + \delta^i_{14})z^j_4 + (\delta^i_{71} + 3\delta^i_{23})z^j_2 + (\delta^i_{47} + 3\delta^i_{26})z^j_1 \\
\phi_{j,i+9} &= 3(\delta^i_{16} + \delta^i_{52})z^j_7 + (\delta^i_{72} + 3\delta^i_{31})z^j_6 + (\delta^i_{67} + 3\delta^i_{35})z^j_5 + (\delta^i_{26} + \delta^i_{51})z^j_4 + (\delta^i_{17} + 3\delta^i_{23})z^j_3 + (\delta^i_{75} + 3\delta^i_{63})z^j_1 \\
\phi_{j,i+12} &= (\delta^i_{57} + 3\delta^i_{14})z^j_6 + 3(\delta^i_{54} + \delta^i_{71})z^j_5 + (\delta^i_{65} + 3\delta^i_{12})z^j_4 + (\delta^i_{76} + 3\delta^i_{42})z^j_3 + 3(\delta^i_{25} + \delta^i_{61})z^j_2 + 3(\delta^i_{27} + \delta^i_{46})z^j_1 \\
\phi_{j,i+15} &= 3(\delta^i_{72} + \delta^i_{46})z^j_7 + 3(\delta^i_{52} + \delta^i_{34})z^j_6 + 3(\delta^i_{37} + \delta^i_{65})z^j_5 + (\delta^i_{54} + 3\delta^i_{23})z^j_4 + (\delta^i_{47} + 3\delta^i_{26})z^j_3 + (\delta^i_{75} + 3\delta^i_{63})z^j_2 \\
\phi_{j,i+18} &= 3(\delta^i_{54} + \delta^i_{17})z^j_7 + (\delta^i_{74} + 3\delta^i_{51})z^j_6 + (\delta^i_{46} + 3\delta^i_{31})z^j_4 + 3(\delta^i_{16} + \delta^i_{43})z^j_3 + (\delta^i_{67} + 3\delta^i_{35})z^j_2 + 3(\delta^i_{73} + \delta^i_{65})z^j_1
\end{aligned}$$

in which geometric constants are defined by

$$\delta^1_{ij} = b_i c_j - b_j c_i \qquad \delta^2_{ij} = c_i a_j - c_j a_i \qquad \delta^3_{ij} = a_i b_j - a_j b_i$$

and values for z^n_j with $n = 1, 2, 3, ..., 8$ are given by

n	z^n_1	z^n_2	z^n_3	z^n_4	z^n_5	z^n_6	z^n_7
1	-1	1	-1	1	-1	-1	1
2	1	-1	1	-1	-1	-1	1
3	1	-1	-1	1	-1	1	-1
4	-1	1	1	-1	-1	1	-1
5	-1	-1	-1	-1	1	1	1
6	1	1	1	1	1	1	1
7	1	1	-1	-1	1	-1	-1
8	-1	-1	1	1	1	-1	-1

(28)

NUMERICAL STUDIES OF THE EXPLICIT PIAN-TONG ELEMENT

The following tables present computer run-times comparing the explicit and numerical generation of stiffness matrices in the Pian-Tong hexahedral element. In the numerical evaluation, under general element distortion, quartic terms involving the natural coordinates appear requiring a 3^{rd}-order Gaussian quadrature rule for exact evaluation as is obtained in the explicit formulation. However, the underintegration utilizing a 2^{nd}-order rule has been found adequate to compute element stiffness coefficients without introducing spurious kinematic modes. The influence of the quartic terms have a negligible influence and a 2^{nd}-order rule is thus considered standard for the 8–node solid hybrid element and is used herein for all numerical integrations. No optimization was attempted in performing the computer implementations of the elements in terms of code preparation or CPU processing options such as vectorization or concurrency. The codes were run on a Hewlett Packard Apollo 400 series workstation in a Unix environment. The standard UNIX profiler Gprof was used to characterize the time spent in performing various operations. In generating the computational profiles, 1000 element stiffness matrices were processed. A description of the procedures used in the codes which account for at least 97% of the computational cost are presented in Table 1. The designation 'main' combines the operations within the main program together with various subroutines which contribute insignificant computational cost. Table 2 details the computational profile for the Pian-Tong element evaluated explicitly and numerically.

Table 1: Subroutine procedures

Name	Description	Name	Description
mxmul	matrix multiplication	gmatrx	explicit computation of G matrix
mxadd	matrix addition	orthop	computation of orthonormal stress modes
invers	matrix inversion	main	main program + minor subroutines

Table 2: Computational profiles of the Pian-Tong (PT) element

PT-Explicit				PT-Numerical			
% time	self seconds	cumulative seconds	procedure name	% time	self seconds	cumulative seconds	procedure name
70.5	39.99	39.99	mxmul	83.5	341.62	341.62	mxmul
18.6	10.56	50.55	gmatrx	7.3	29.90	371.52	mxadd
8.9	5.03	55.58	orthop	6.9	28.43	399.95	invers
2.0	1.12	56.70	main	2.3	9.42	409.37	main

The computational profiles quantify the different characteristics of the explicit and numerical versions of the Pian-Tong element. As shown, the computational cost of both the explicit and numerical versions is mostly spent in matrix multiplication and addition consuming 70.5 % and 90.8 % of the processing time, respectively. Comparing total computer run–times, the explicit version requires only 13.9 % of the computational cost as that consumed in the underintegrated numerical evaluation. Not shown in the tables, the exact integration of the quartic terms in the numerical version using 3^{rd}-order Gaussian quadrature results in a run-time of 1167.4 seconds. Compared to this the explicit formulation requires only 4.9 % of the computational expense.

NONLINEAR ELEMENT STIFFNESS DEFINITION

The extension to nonconstant material properties requires that the compliance matrix be interpolated over the element domain. For illustration, the Pian-Sumihara quadrilateral element is selected[6]. For the plane element under study a bilinear isoparametric field is sufficient for interpolating compliance properties; however, the derived $\mathbf{D}$ matrix is a nonlinear function of $\mathbf{S}$ thus requiring a higher order interpolation. A quadratic isoparametric field is adopted in which the material matrices are computed at the stress recovery or material evaluation points depicted in Figure 2. Thus, at arbitrary points over the element domain $\mathbf{D} = \bar{\mathbf{S}}^{-1/2}$ and the interpolation results in the relationship $\bar{\mathbf{S}} = \mathbf{S}$ being strictly valid at the recovery points and approximate elsewhere. The accuracy of this approximation is discussed later in Remark I.

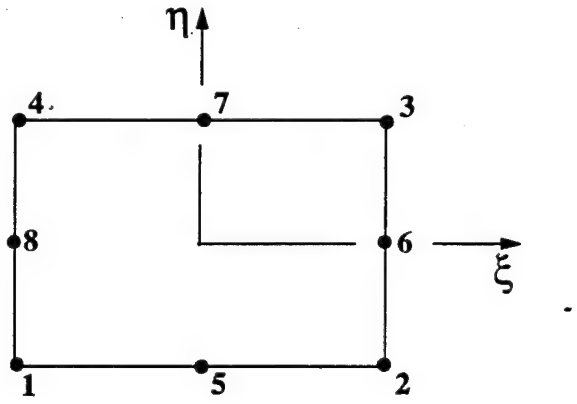

Figure 2. Evaluation points used for material interpolation.

The interpolation is given by

$$\Omega(\xi,\eta) = \sum_{i=1}^{8} N_i(\xi\eta)\Omega_i \tag{29}$$

where Ω_i represents the material $\mathbf{D}$ and $\mathbf{D}^{-1}$ matrices computed at the i^{th} stress recovery point and N_i are the associated quadratic–order isoparametric shape functions. Interpolation of the material matrices over the element domain may be expressed as

$$\Omega(\xi,\eta) = \mathbf{A}_1 + \mathbf{A}_2\xi + \mathbf{A}_3\eta + \mathbf{A}_4\xi^2 + \mathbf{A}_5\eta^2 + \mathbf{A}_6\xi\eta + \mathbf{A}_7\xi^2\eta + \mathbf{A}_8\xi\eta^2 \tag{30}$$

where the constant matrices, $\mathbf{A}_i$, are given by

$$\begin{Bmatrix} \mathbf{A}_1 \\ \mathbf{A}_2 \\ \mathbf{A}_3 \\ \mathbf{A}_4 \\ \mathbf{A}_5 \\ \mathbf{A}_6 \\ \mathbf{A}_7 \\ \mathbf{A}_8 \end{Bmatrix} = \frac{1}{4} \begin{bmatrix} -1 & -1 & -1 & -1 & 2 & 2 & 2 & 2 \\ & & & & & 2 & & -2 \\ & & & & -2 & & 2 & \\ 1 & -1 & 1 & -1 & & & & \\ 1 & 1 & 1 & 1 & -2 & & -2 & \\ -1 & -1 & 1 & 1 & & 2 & & -2 \\ -1 & -1 & 1 & 1 & 2 & & -2 & \\ -1 & 1 & 1 & -1 & & -2 & & 2 \end{bmatrix} \begin{Bmatrix} \Omega_1 \\ \Omega_2 \\ \Omega_3 \\ \Omega_4 \\ \Omega_5 \\ \Omega_6 \\ \Omega_7 \\ \Omega_8 \end{Bmatrix} \tag{31}$$

Following the procedure outlined above in equations (7) through (18), substitution of (7) into (5) based on the distribution represented by equation (30) yields the flexibility matrix as

$$\mathbf{H} = \int_{-1}^{1} \int_{-1}^{1} [|\mathbf{J}| \bar{\mathbf{P}}^T \mathbf{D}^T \mathbf{S} \mathbf{D} \bar{\mathbf{P}}] d\xi d\eta \tag{32}$$

where, from the definition of $\mathbf{D}$ and the symmetry of both $\mathbf{S}$ and $\mathbf{D}$ we obtain

$$\mathbf{D}^T \mathbf{S} \mathbf{D} = \bar{\mathbf{S}}^{-1/2} \mathbf{S} \bar{\mathbf{S}}^{-1/2} = \mathbf{S} \bar{\mathbf{S}}^{-1} \approx \mathbf{I} \tag{33}$$

The approximation rapidly approaches an identity as the interpolation order of $\mathbf{D}$ increases and as the variation of material properties over the element diminishes. The flexibility matrix is thereby closely approximated by

$$\mathbf{H} \approx \int_{-1}^{1} \int_{-1}^{1} [|\mathbf{J}| \bar{\mathbf{P}}^T \bar{\mathbf{P}}] d\xi d\eta \tag{34}$$

A second field transformation uses equation (34) to define a weighted inner product for use in a Gram-Schmidt procedure to generate an orthonormal spanning set of stress modes, $\mathbf{P}^*$. This modal set is formed as a special linear combination of the modes present in $\bar{\mathbf{P}}$ and constitutes an alternative basis set which spans the original stress space. The weighted inner product is therefore defined as

$$< \bar{\mathbf{P}}_i, \bar{\mathbf{P}}_j > = \int_{-1}^{1} \int_{-1}^{1} [|\mathbf{J}| \bar{\mathbf{P}}_i^T \bar{\mathbf{P}}_j] d\xi d\eta = \delta_{ij} \tag{35}$$

where δ_{ij} is the Kronecker delta function. The linear combination yielding a sequence of orthogonal stress modes is given by

$$\mathbf{V}_i = \begin{cases} \bar{\mathbf{P}}_i & i = 1 \\ \bar{\mathbf{P}}_i - \sum_{j=1}^{i-1} < \mathbf{P}_j^*, \bar{\mathbf{P}}_i > \mathbf{P}_j^* & i > 1 \end{cases} \tag{36}$$

which are normalized to form basis vectors, $\mathbf{P}_i^*$, as

$$\mathbf{P}_j^* = < \mathbf{V}_i, \mathbf{V}_i >^{-1/2} \mathbf{V}_i \tag{37}$$

In the definition of $\bar{\mathbf{P}}$, the $\mathbf{D}^{-1}$ matrix is interpolated according to (30) and carried into the subsequent orthonormalization of assumed stress modes. For the present study, however, a simplification is adopted wherein the $\mathbf{D}$ matrix is interpolated according to equation (30) while its inverse is obtained from an area average obtained by integrating over the element domain. This operation is not required but is utilized in the present study to simplify the expressions for the orthonormalized stress modes, $\mathbf{P}^*$, while maintaining an adequate approximation for the material properties. The inverse is thus defined as

$$\mathbf{D}^{-1} = \left[\frac{1}{4} \int_{-1}^{1} \int_{-1}^{1} \mathbf{D}(\xi, \eta) d\xi d\eta \right]^{-1} \tag{38}$$

and the relationship

$$\mathbf{D}(\xi, \eta) \mathbf{D}^{-1} \approx \mathbf{I} \tag{39}$$

is satisfied in an integral sense for nonconstant material properties and pointwise for constant properties over the element domain. Substitution of $\mathbf{P}^*$ into equation (34) yields by definition

$$\mathbf{H} = \int_{-1}^{1}\int_{-1}^{1} [|\mathbf{J}|\mathbf{P}^{*T}\mathbf{P}^*]d\xi d\eta \equiv \mathbf{I} \tag{40}$$

Repeating the above relations, the new basis for the element stress field is given by

$$\mathbf{P} = \mathbf{D}\mathbf{P}^* \tag{41}$$

and the expression for the element stiffness matrix reduces to

$$\mathbf{K} = \mathbf{G}^T\mathbf{G} \tag{42}$$

Separating out the Jacobian determinant from the isoparametric strains as

$$\mathbf{B} = \frac{1}{|\mathbf{J}|}\mathbf{B}^*(\xi,\eta,\zeta) \tag{43}$$

and substituting (41) and (43) into (6) the $\mathbf{G}$ matrix definition becomes

$$\mathbf{G} = \int_{-1}^{1}\int_{-1}^{1} [\mathbf{P}^{*T}\mathbf{D}\mathbf{B}^*]d\xi d\eta \tag{44}$$

The absence of the Jacobian determinant in the denominator permits a direct derivation of algebraic expressions for the $\mathbf{G}$ matrix coefficients which incorporate a nonconstant field of material properties over the element domain. The explicit form of the element stiffness matrix is then obtained from equation (42).

NONLINEAR PIAN-SUMIHARA QUADRILATERAL ELEMENT

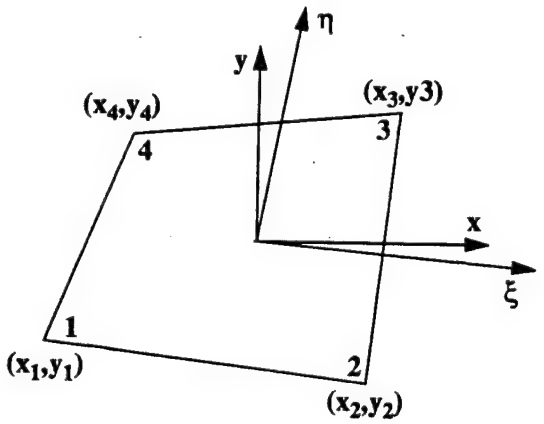

Figure 3. Quadrilateral element configuration.

The configuration of the Pian-Sumihara element and node numbering are depicted in Figure 3. The displacement functions $\mathbf{u}_q$ are given by

$$\mathbf{u}_q = \begin{pmatrix} u_q \\ v_q \end{pmatrix} = \frac{1}{4}\sum_{i=1}^{4}(1+\xi_i\xi)(1+\eta_i\eta)\begin{pmatrix} u_i \\ v_i \end{pmatrix} \tag{45}$$

As detailed in Reference [6], stresses are defined in natural or tensorial coordinates and incompatible displacement modes are introduced to complete the quadratic order of the assumed isoparametric displacement field. These modes are condensed *a priori* into the element formulation through constraint conditions on the

assumed stress modes.

The tensorial stress field is transformed to physical or Cartesian coordinates using Jacobians computed at the element centroid as

$$\sigma^{kl} = (J_o)^k_i (J_o)^l_j \tau^{ij} \tag{46}$$

Performing the initial transformation of stresses given by (7) results in the Cartesian stress field given by

$$\boldsymbol{\sigma} = [\sigma_x, \sigma_y, \tau_{xy}]^T = \bar{\mathbf{P}}\boldsymbol{\beta} \tag{47}$$

where

$$\bar{\mathbf{P}} = \begin{bmatrix} 1 & & & c_{11}\xi & c_{12}\eta \\ & 1 & & c_{21}\xi & c_{22}\eta \\ & & 1 & c_{31}\xi & c_{32}\eta \end{bmatrix} \tag{48}$$

and the coefficients c_{ij} are obtained from the product of $\mathbf{D}^{-1}$ and a transformation matrix relating tensorial stresses to Cartesian components. This relationship is given by

$$[c_{ij}] = \mathbf{D}^{-1}\boldsymbol{\Gamma} = \begin{bmatrix} \bar{d}_{11} & \bar{d}_{12} & \\ \bar{d}_{21} & \bar{d}_{22} & \\ & & \bar{d}_{33} \end{bmatrix} \begin{bmatrix} a_2^2 & a_1^2 \\ b_2^2 & b_1^2 \\ a_2 b_2 & a_1 b_1 \end{bmatrix}$$

The geometric parameters a_i and b_i are obtained from the mapping between physical and natural coordinates given by

$$\begin{aligned} x &= a_0 + a_1\xi + a_2\eta + a_3\xi\eta \\ y &= b_0 + b_1\xi + b_2\eta + b_3\xi\eta \end{aligned} \tag{49}$$

where

$$\begin{bmatrix} a_0 & b_0 \\ a_1 & b_1 \\ a_2 & b_2 \\ a_3 & b_3 \end{bmatrix} = \frac{1}{4} \begin{bmatrix} 1 & 1 & 1 & 1 \\ -1 & 1 & 1 & -1 \\ -1 & -1 & 1 & 1 \\ 1 & -1 & 1 & -1 \end{bmatrix} \begin{bmatrix} x_1 & y_1 \\ x_2 & y_2 \\ x_3 & y_3 \\ x_4 & y_4 \end{bmatrix}$$

The weighted orthonormalized stress modes are obtained as

$$\mathbf{P}^* = \begin{bmatrix} p^*_{13} & 0 & 0 & p^*_{42}\xi + p^*_{43} & p^*_{51}\eta + p^*_{52}\xi + p^*_{53} \\ 0 & p^*_{26} & 0 & p^*_{45}\xi + p^*_{46} & p^*_{54}\eta + p^*_{55}\xi + p^*_{56} \\ 0 & 0 & p^*_{39} & p^*_{48}\xi + p^*_{49} & p^*_{57}\eta + p^*_{58}\xi + p^*_{59} \end{bmatrix} \tag{50}$$

where the stress mode coefficients, p^*_{ij}, are presented in Appendix II.

Given the following constants arising from the regular structure of the strain modes

$$\begin{aligned} e_{1j} &= b_2 z_1^j - b_1 z_2^j \qquad e_{4j} = a_1 z_2^j - a_2 z_1^j \\ e_{2j} &= b_3 z_1^j - b_1 z_3^j \qquad e_{5j} = a_1 z_3^j - a_3 z_1^j \\ e_{3j} &= b_2 z_3^j - b_3 z_2^j \qquad e_{6j} = a_3 z_2^j - a_2 z_3^j \end{aligned} \qquad \textit{where}$$

j	z_1^j	z_2^j	z_3^j
1	-1	-1	1
2	1	-1	-1
3	1	1	1
4	-1	1	-1

(51)

and the general form for each stress mode given by

$$\mathbf{P}^*_i = \begin{Bmatrix} p_{i1}\eta + p_{i2}\xi + p_{i3} \\ p_{i4}\eta + p_{i5}\xi + p_{i6} \\ p_{i7}\eta + p_{i8}\xi + p_{i9} \end{Bmatrix} \tag{52}$$

the integration of (44) yields explicit expressions for the components of the **G** matrix. The expressions are based on the most general form of orthonormalized stress modes in which most terms are zero for the simpler modes and the constants $(d_{ij})_k$ are elements of the **D** matrix computed at the k^{th} evaluation point. In addition, for constant material properties, if all $(d_{ij})_k$ terms are discarded for $k > 1$ the resulting

expressions reduce to an explicit form of the linear–elastic Pian-Sumihara element. The components g_{ij} with $i = 1, 2, 3, ..., 5$ and $j = 1, 2, 3, 4$ are given by

$$
\begin{aligned}
g_{i,2j-1} \;=\; & (p^*_{i1}\{(e_{1j}[(d_{11})_7 + 3(d_{11})_3] + e_{3j}[(d_{11})_4 + 3(d_{11})_1 + 9(d_{11})_5/5] + (d_{11})_6 e_{2j}\} + \\
& p^*_{i2}\{(e_{1j}[(d_{11})_8 + 3(d_{11})_2] + e_{2j}[(d_{11})_5 + 3(d_{11})_1 + 9(d_{11})_4/5] + (d_{11})_6 e_{3j}\} + \\
& p^*_{i3}\{(e_{2j}[(d_{11})_8 + 3(d_{11})_2] + e_{3j}[(d_{11})_7 + 3(d_{11})_3] + 3e_{1j}[(d_{11})_5 + (d_{11})_4 + 3(d_{11})_1]\} + \\
& p^*_{i4}\{(e_{1j}[(d_{12})_7 + 3(d_{12})_3] + e_{3j}[(d_{12})_4 + 3(d_{12})_1 + 9(d_{12})_5/5] + e_{2j}(d_{12})_6\} + \\
& p^*_{i5}\{(e_{1j}[(d_{12})_8 + 3(d_{12})_2] + e_{2j}[(d_{12})_5 + 3(d_{12})_1 + 9(d_{12})_4/5] + e_{3j}(d_{12})_6\} + \\
& p^*_{i6}\{(e_{3j}[(d_{12})_7 + 3(d_{12})_3] + e_{2j}[(d_{12})_8 + 3(d_{12})_2] + 3e_{1j}[(d_{12})_5 + (d_{12})_4 + 3(d_{12})_1]\} + \\
& p^*_{i7}\{(e_{4j}[(d_{33})_7 + 3(d_{33})_3] + e_{6j}[(d_{33})_4 + 3(d_{33})_1 + 9(d_{33})_5/5] + e_{5j}(d_{33})_6\} + \\
& p^*_{i8}\{(e_{4j}[(d_{33})_8 + 3(d_{33})_2] + e_{5j}[(d_{33})_5 + 3(d_{33})_1 + 9(d_{33})_4/5] + e_{6j}(d_{33})_6\} + \\
& p^*_{i9}\{(e_{5j}[(d_{33})_8 + 3(d_{33})_2] + e_{6j}[(d_{33})_7 + 3(d_{33})_3] + 3e_{4j}[(d_{33})_5 + (d_{33})_4 + 3(d_{33})_1]\})/9
\end{aligned}
\tag{53}
$$

$$
\begin{aligned}
g_{i,2j} \;=\; & (p^*_{i1}\{(e_{4j}[(d_{12})_7 + 3(d_{12})_3] + e_{6j}[(d_{12})_4 + 3(d_{12})_1 + 9(d_{12})_5/5] + (d_{12})_6 e_{5j}\} + \\
& p^*_{i2}\{(e_{4j}[(d_{12})_8 + 3(d_{12})_2] + e_{5j}[(d_{12})_5 + 3(d_{12})_1 + 9(d_{12})_4/5] + (d_{12})_6 e_{6j}\} + \\
& p^*_{i3}\{(e_{5j}[(d_{12})_8 + 3(d_{12})_2] + e_{6j}[(d_{12})_7 + 3(d_{12})_3] + 3e_{4j}[(d_{12})_5 + (d_{12})_4 + 3(d_{12})_1]\} + \\
& p^*_{i4}\{(e_{4j}[(d_{22})_7 + 3(d_{22})_3] + e_{6j}[(d_{22})_4 + 3(d_{22})_1 + 9(d_{22})_5/5] + e_{5j}(d_{22})_6\} + \\
& p^*_{i5}\{(e_{4j}[(d_{22})_8 + 3(d_{22})_2] + e_{5j}[(d_{22})_5 + 3(d_{22})_1 + 9(d_{22})_4/5] + e_{6j}(d_{22})_6\} + \\
& p^*_{i6}\{(e_{6j}[(d_{22})_7 + 3(d_{22})_3] + e_{5j}[(d_{22})_8 + 3(d_{22})_2] + 3e_{4j}[(d_{22})_5 + (d_{22})_4 + 3(d_{22})_1]\} + \\
& p^*_{i7}\{(e_{1j}[(d_{33})_7 + 3(d_{33})_3] + e_{3j}[(d_{33})_4 + 3(d_{33})_1 + 9(d_{33})_5/5] + e_{2j}(d_{33})_6\} + \\
& p^*_{i8}\{(e_{1j}[(d_{33})_8 + 3(d_{33})_2] + e_{2j}[(d_{33})_5 + 3(d_{33})_1 + 9(d_{33})_4/5] + e_{3j}(d_{33})_6\} + \\
& p^*_{i9}\{(e_{2j}[(d_{33})_8 + 3(d_{33})_2] + e_{3j}[(d_{33})_7 + 3(d_{33})_3] + 3e_{1j}[(d_{33})_5 + (d_{33})_4 + 3(d_{33})_1]\})/9
\end{aligned}
$$

NUMERICAL STUDIES OF THE EXPLICIT PIAN-SUMIHARA ELEMENT

Computer codes were generated to assess element computational characteristics. A description of the procedures used in the codes are presented in Table 3. The designation 'main' combines the operations within the main program together with various minor subroutines which contribute insignificant computational cost. No optimization was attempted in terms of code preparation or CPU processing options such as vectorization or concurrency. The codes were run on a Hewlett Packard Apollo 400 series workstation in a Unix environment. The standard Unix profiler Gprof was used to characterize the time spent in performing various operations. Table 4 presents computational profiles and computer run-times comparing the explicit and numerical generation of stiffness matrices in the nonlinear Pian-Sumihara quadrilateral element. An additional comparison is made to a 4–node displacement–based element incorporating incompatible displacement modes which is presented in Table 5. The incompatible modes are based on quadratic functions and modified using a technique presented in Reference [8] to identically satisfy the strong form of the patch test for incompatible elements. A 2^{nd}-order Gaussian quadrature rule was used for all numerical evaluations in generating computational profiles. In generating the computational profiles, 10,000 element stiffness matrices were processed.

Table 3: Subroutine procedures

Name	Description	Name	Description
mxmul	matrix multiplication	gmatrx	explicit computation of **G** matrix
mxadd	matrix addition	orthop	computation of orthonormal stress modes
invers	matrix inversion	spectrl	spectral decomposition of **S** matrix
statc	static condensation	main	matrix main program + minor subroutines

Table 4: Computational profiles of the nonlinear Pian-Sumihara (PS) element

PS-Explicit				PS-Numerical			
% time	self seconds	cumulative seconds	procedure name	% time	self seconds	cumulative seconds	procedure name
32.76	16.55	16.55	spectrl	75.46	109.09	109.09	mxmul
30.09	15.20	31.75	mxmul	9.26	13.38	122.47	mxadd
21.71	10.97	42.72	gmatrx	6.50	9.39	131.86	invers
3.17	1.60	44.32	orthop	8.78	12.71	144.57	main
12.27	6.20	50.52	main				

Table 5: Computational profile of incompatible displacement-based element

D–Based			
% time	self seconds	cumulative seconds	procedure name
71.6	160.82	160.82	mxmul
13.0	29.18	190.00	mxadd
11.0	24.63	214.63	statc
4.4	10.12	224.75	main

The computational profiles quantify the different characteristics of the explicit and numerical versions of the nonlinear Pian-Sumihara element. In the explicit version, the eight spectral decompositions of the compliance matrix consume the greatest amount of computational cost (32.76%) while matrix multiplications constitute most of the computations in the numerical version (75.46%). The computational profile of the explicit version shows that the operations involved in forming the orthonormal stress modes is insignificant (3.17%) while the formation of the **G** matrix consumes 21.71% of the cost. The final evaluation of equation (24), which is the only matrix operation performed in the explicit version, constitutes fully 30% of the cost in forming the element stiffness matrix. Comparing total cost, the explicit version requires only 34.95% of the processing time as the numerical evaluation and only 22.48% of the cost required in the incompatible displacement–based formulation. While this represents a significant reduction in processing cost, application of the developed methodology may be expected to show greater reductions in 3–D and higher–order hybrid element formulations. This issue is discussed in Remark II.

A second demonstration is made to show the accuracy of the nonlinear material representation in the explicit formulation. Because the basic computational characteristics have been shown above, a cantilevered beam under plane stress is solved where the material properties are not a function of the stress/strain state but instead vary along the length of the beam. Such a problem is uncommon but serves to illustrate the representation of material property variation in the clearest manner. The beam was analyzed using a coarse model of 5 elements. Two different mesh configurations were used as shown in Figure 4; a uniform mesh was adopted to assess optimum element performance and a nonuniform mesh was used to assess distortion sensitivity to the simplifications currently incorporated in the explicit derivation. For simplicity, isotropic material properties were assumed with a linear variation of modulus as depicted in Figure 5.

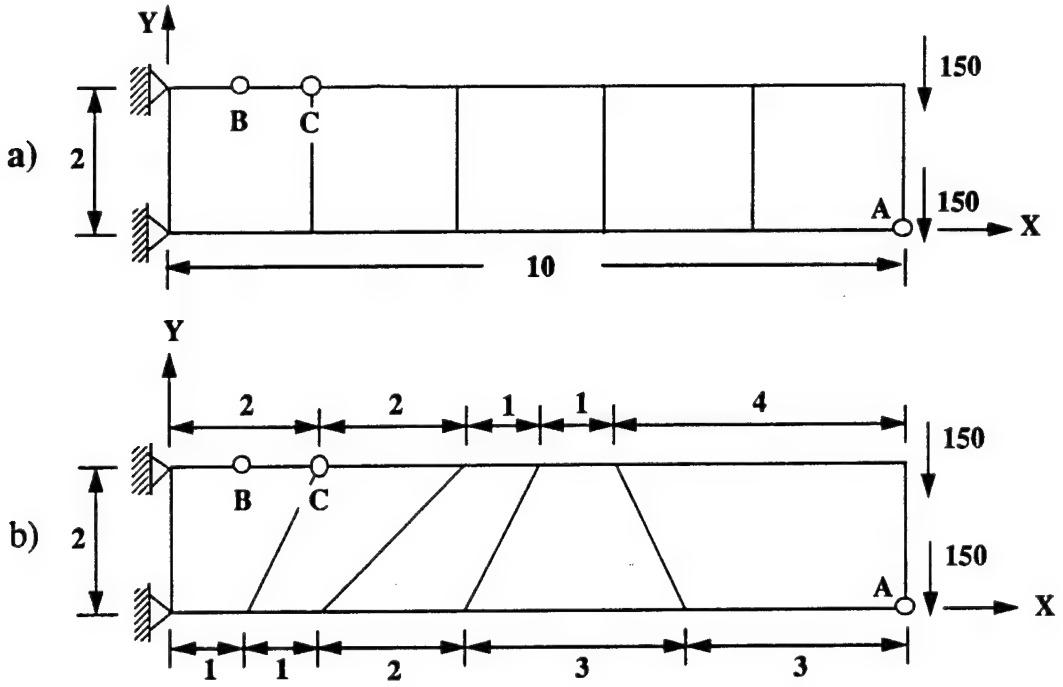

Figure 4. Cantilevered beam configurations: a) uniform mesh, b) distorted mesh.

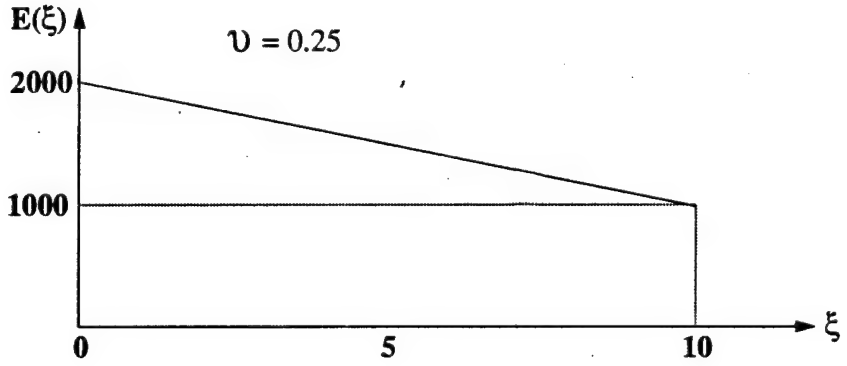

Figure 5. Assumed linear variation in Young's modulus along beam length.

Table 6 depict solutions for the explicit and numerical hybrid element formulations together with results using an incompatible displacement–based element.

Table 6. Deflection of nonlinear cantilevered beam under end shear loading.

a)Uniform Mesh				b) Distorted Mesh			
Elements	v_a	$\sigma_{x(b)}$	$\sigma_{x(c)}$	Elements	v_a	$\sigma_{x(b)}$	$\sigma_{x(c)}$
PS-Explicit	-88.7	4045	3587	PS-Explicit	-86.1	4048	3728
PS-Numerical	-89.1	4050	3600	PS-Numerical	-90.1	4047	3735
D–Based	-89.0	4050	3586	D–Based	-89.9	3276	3079
Exact	-90.4	4043	3601	Exact	-90.4	4043	3601

Comparing the above results show an excellent agreement between the explicit and numerical hybrid el-

ement formulations for both meshes; a small departure is seen in the tip deflection prediction in the explicit formulation using the irregular mesh due to the incorporated simplifications. The incompatible displacement–based element demonstrates good results for both stresses and displacements using a uniform mesh; however, in the distorted mesh, stress recovery is severely compromised. In general, the greater computational cost of the displacement–based element makes it unappealing.

REMARK I

An important aspect of the above development involves the collocation error of the **D** matrix over the element domain using quadratic isoparametric shape functions. Because this matrix is computed as the square root of the material stiffness matrix, the individual components in **D** are interpolated to yield the approximate relation given above in equation (39). A formal error estimate may be derived for arbitrary variation of material properties and order of collocation polynomials; however, a clearer illustration may be given by assuming a specific variation in the compliance matrix components as a function of a single coordinate, thus simplifying the error analysis to a one–dimensional demonstration. A linear function is selected in which a parameter, θ, is used to set the magnitude of variation in the material component denoted by C_0. The resulting square root distribution is given by

$$f(\xi) = C_0^{1/2}[1 + \theta(1 + \xi)]^{1/2}$$

The values of $f(\xi)$ at the evaluation points along $\xi \in (-1, 1)$ are depicted in Figure 6.

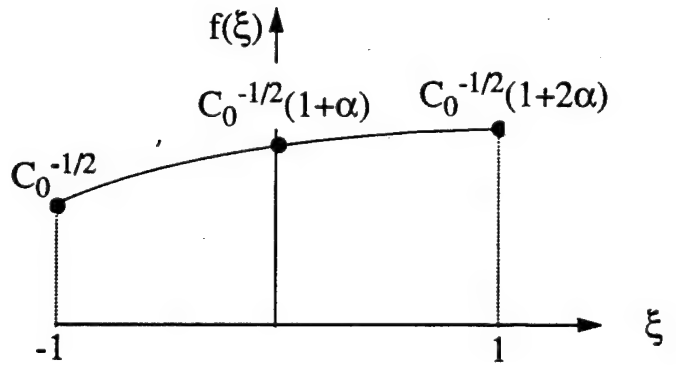

Figure 6. Variation in material properties over segment.

The quadratic isoparametric interpolation is given by

$$p(\xi) = C_0^{1/2}\{(1 + \theta)^{1/2} + \frac{1}{2}[(1 + 2\theta)^{1/2}]\xi + \frac{1}{2}[1 - 2(1 + \theta)^{1/2} + (1 + 2\theta)^{1/2}]\xi^2\}$$

An error measure for point evaluation may be given by

$$E_p = \frac{|f(\xi) - p(\xi)|}{f(\xi)}$$

A second error measure is associated with the difference between the integrated areas computed by the exact solution and the quadratic collocation. The integral of the exact distribution is given by

$$F(\xi) = \int_{-1}^{1} f(\xi)d\xi = \frac{2}{3\theta}C_0{}^{1/2}[(2\theta + 1)^{3/2} - 1]$$

while the integral of the collocated function is given by

$$P(\xi) = \int_{-1}^{1} p(\xi)d\xi = \frac{1}{3}C_0{}^{1/2}[1 + 4(1 + \theta)^{1/2} + (1 + 2\theta)^{1/2}]$$

An error measure for the integral evaluation may be given by

$$E_i = \frac{|F(\xi) - P(\xi)|}{F(\xi)}$$

Table 7 details error measures at the points of maximum expected error and the integrated error between the two assumed functions.

Table 7. Error measures for point and integral evaluation of material property interpolation.

θ	$E_p(\xi = -\frac{1}{2})$	$E_p(\xi = \frac{1}{2})$	E_i
0.00	0.0	0.0	0.0
0.01	2.287E-6	2.262E-6	5.005E-9
0.05	2.603E-4	2.467E-4	2.683E-6
0.1	1.862E-3	1.681E-3	3.581E-5
0.2	1.211E-2	1.003E-2	4.109E-4
0.3	3.384E-2	2.606E-2	1.542E-3
0.4	6.739E-2	4.871E-2	3.710E-3
0.5	1.120E-1	7.658E-2	7.048E-3
0.6	1.664E-1	1.083E-1	1.158E-2
0.7	2.292E-1	1.429E-1	1.728E-2
0.8	2.993E-1	1.794E-1	2.406E-2
0.9	3.754E-1	2.171E-1	3.184E-2
1.0	4.565E-1	2.555E-1	4.051E-2

The above table indicates that the maximum point collocation error for a 40% variation in modulus ($\theta = 0.2$) over the segment is just over 1%. At $\theta = 0.5$, corresponding to a 100% variation in material properties, the point error increases to 11.2%. However, even when the properties vary by a factor of 3 ($\theta = 1.0$) over the segment, the integrated error, E_i, is still small, on the order of 4.05%.

REMARK II

With stresses assumed in natural coordinates, the procedure described herein may be applied directly. For higher–order elements, the approach of assuming tensorial stresses with a contravariant transformation using centroidal Jacobians to obtain Cartesian stresses is inaccurate and neccessitates a formulation based on stresses assumed *a priori* in Cartesian coordinates. For assumed Cartesian stress fields, a fully explicit derivation may become overly cumbersome and computationally disadvantageous. In such cases the basic methodology is applied but numerical quadrature of the scalar integrals arising in the weighted inner product and computation of **G**-matrix components is advocated. In higher–order elements, the reduction in computational cost afforded by adapting the present methodology is expected to be significantly greater than that demonstrated for the 4–node quadrilateral element due to the larger order of the constituent matrices. The computational savings result from eliminating the cost of forming and inverting the complementary energy matrix, **H**, and by replacing the numerical quadrature of large–order matrix products by the quadrature of a small set of scalar integrals.

CONCLUSION

The developed methodology for deriving explicit hybrid element stiffness matrices has been applied to the linear–elastic Pian-Tong 8-node solid continuum element and has been extended to develop an explicit formulation for the nonlinear–elastic Pian-Sumihara quadrilateral element. The 3–D element formulation incorporates a complex set of higher–order stress modes yet, through application of a simplifying methodology, has been shown to permit a straightforward derivation of explicit algebraic expressions for element stiffness

coefficients. In comparison with an underintegrated numerical version of the element using a 2^{nd}-order Gaussian quadrature rule, the explicit derivation required less than 14 % of the computational cost in forming element stiffness matrices. If an exact integration is required in the numerical version, the explicit derivation demonstrates a 20–fold increase in computational efficiency. The enhancement of computational efficiency of hybrid element formulations for nonlinear analysis has been demonstrated using the 4–node Pian-Sumihara quadrilateral element to derive explicit formulations accommodating nonconstant material properties. The derivation of an explicit element stiffness matrix has been shown to substantially reduce the computational cost in nonlinear analysis. The developed methodology is completely generic and may be applied to any hybrid element formulation to reduce the computational cost in linear and nonlinear applications. In the application to higer–order element formulations, an assumption of Cartesian stresses lead most efficiently to a combination of numerical evaluation of the scalar integrals involved in the orthonormalization process and in the integration of of various integrals required in determining components of the **G** matrix. All other integrations may be performed analytically. The increase in efficiency demonstrated with a linear–order hybrid element is expected to be even more pronounced in higher–order element formulations due to the elimination of forming and inverting the complementary energy matrix and by replacing the numerical quadrature of large–order matrix products with the analytical/numerical integration of a relatively small set of scalar integrals. The application of the above methodology can be expected to find general application in hybrid and mixed element formulations and provide a significant reduction in computational cost in generating element stiffness matrices for linear and nonlinear analysis.

APPENDIX I

SPECTRAL DECOMPOSITION

The spectral decomposition of an orthotropic material compliance matrix is given by

$$D = S^{-1/2} = C^{1/2} \quad ; \quad C^{1/2} = Q\Lambda^{1/2}Q^T$$

where the C and D matrix are given for a 2–D orthotropic material as

$$C = \begin{bmatrix} c_{11} & c_{12} & 0 \\ c_{12} & c_{22} & 0 \\ 0 & 0 & c_{33} \end{bmatrix} \qquad D = \begin{bmatrix} d_{11} & d_{12} & 0 \\ d_{12} & d_{22} & 0 \\ 0 & 0 & d_{33} \end{bmatrix}$$

The eigenvalues are computed as

$$\begin{aligned} \varphi_1 &= (-\sqrt{c_{22}^2 - 2c_{11}c_{22} + 4c_{12}^2 + c_{11}^2} + c_{22} + c_{11})/2 \\ \varphi_2 &= (\sqrt{c_{22}^2 - 2c_{11}c_{22} + 4c_{12}^2 + c_{11}^2} + c_{22} + c_{11})/2 \\ \varphi_3 &= c_{33} \end{aligned}$$

yielding the $\Lambda^{1/2}$ matrix as

$$\Lambda^{1/2} = diag[\varphi_1^{1/2}, \varphi_2^{1/2}, \varphi_3^{1/2}]$$

The Q matrix is defined as

$$Q = [\Phi_1|\Phi_2|\Phi_3]$$

where the eigenvectors are given by

$$\bar{\Phi}_1 = \begin{Bmatrix} c_{12} \\ \varphi_1 - c_{11} \\ 0 \end{Bmatrix}, \quad \bar{\Phi}_2 = \begin{Bmatrix} \varphi_2 - c_{22} \\ c_{12} \\ 0 \end{Bmatrix}, \quad \bar{\Phi}_3 = \begin{Bmatrix} 0 \\ 0 \\ c_{33} \end{Bmatrix}$$

and normalized as

$$N_i = (\bar{\Phi}_i^T \bar{\Phi}_i)^{-1/2}$$

$$\Phi_i = N_i \bar{\Phi}_i$$

The computation of the 3-D distributing matrix using the symmetric C matrix for an orthotropic material is performed as follows.

$$C = \begin{bmatrix} c_{11} & c_{12} & c_{13} & 0 & 0 & 0 \\ c_{12} & c_{22} & c_{23} & 0 & 0 & 0 \\ c_{13} & c_{23} & c_{33} & 0 & 0 & 0 \\ 0 & 0 & 0 & c_{44} & 0 & 0 \\ 0 & 0 & 0 & 0 & c_{55} & 0 \\ 0 & 0 & 0 & 0 & 0 & c_{66} \end{bmatrix} \quad D = \begin{bmatrix} d_{11} & d_{12} & d_{13} & 0 & 0 & 0 \\ d_{12} & d_{22} & d_{23} & 0 & 0 & 0 \\ d_{13} & d_{23} & d_{33} & 0 & 0 & 0 \\ 0 & 0 & 0 & d_{44} & 0 & 0 \\ 0 & 0 & 0 & 0 & d_{55} & 0 \\ 0 & 0 & 0 & 0 & 0 & d_{66} \end{bmatrix}$$

In the spectral decomposition, eigenvalues are obtained as

$$\begin{aligned} \varphi_1 &= t_1 + t_2 - a/3 & \qquad \varphi_4 &= c_{44} \\ \varphi_2 &= (-(t_1+t_2) - 2a/3 + \sqrt{-3}(t_1 - t_2))/2 & \qquad \varphi_5 &= c_{55} \\ \varphi_3 &= (-(t_1+t_2) - 2a/3 - \sqrt{-3}(t_1 - t_2))/2 & \qquad \varphi_6 &= c_{66} \end{aligned}$$

where

$$\begin{aligned} t_1 &= (r + \sqrt{q^3 + r^2})^{1/3} \\ t_2 &= (r - \sqrt{q^3 + r^2})^{1/3} \\ q &= b/3 - a^2/9 \;\; ; \;\; r = (ab - 3c)/6 - a^3/27 \\ a &= -(c_{33} + c_{22} + c_{11}) \\ b &= (c_{22} + c_{11})c_{33} - c_{23}^2 - c_{13}^2 + c_{11}c_{22} - c_{12}^2 \\ c &= (c_{11}c_{22} + c_{12}^2)c_{33} + c_{11}c_{23}^2 - 2c_{12}c_{13}c_{23} + c_{13}^2 c_{22} \end{aligned}$$

yielding the $\Lambda^{1/2}$ matrix as

$$\Lambda^{1/2} = diag[\varphi_1^{1/2}, \varphi_2^{1/2}, \varphi_3^{1/2}, \varphi_4^{1/2}, \varphi_5^{1/2}, \varphi_6^{1/2}]$$

The Q matrix is given by

$$Q = [\Phi_1 | \Phi_2 | \Phi_3 | \Phi_4 | \Phi_5 | \Phi_6]$$

where the eigenvectors are given by

$$\bar{\Phi}_1 = \begin{Bmatrix} (c_{22} - \varphi_1)(c_{33} - \varphi_1) - c_{23}^2 \\ c_{13}c_{23} - c_{12}(c_{33} - \varphi_1) \\ c_{12}c_{23} - c_{13}(c_{22} - \varphi_1) \\ 0 \\ 0 \\ 0 \end{Bmatrix}, \quad \bar{\Phi}_2 = \begin{Bmatrix} c_{13}c_{23} - c_{12}(c_{33} - \varphi_2) \\ (c_{11} - \varphi_2)(c_{33} - \varphi_2) - c_{13}^2 \\ c_{12}c_{13} - c_{23}(c_{11} - \varphi_2) \\ 0 \\ 0 \\ 0 \end{Bmatrix}$$

$$\bar{\Phi}_3 = \begin{Bmatrix} c_{12}c_{23} - c_{13}(c_{22} - \varphi_3) \\ c_{12}c_{13} - c_{23}(c_{11} - \varphi_3) \\ (c_{11} - \varphi_3)(c_{22} - \varphi_3) - c_{12}^2 \\ 0 \\ 0 \\ 0 \end{Bmatrix}, \bar{\Phi}_4 = \begin{Bmatrix} 0 \\ 0 \\ 0 \\ c_{44} \\ 0 \\ 0 \end{Bmatrix}, \quad \bar{\Phi}_5 = \begin{Bmatrix} 0 \\ 0 \\ 0 \\ 0 \\ c_{55} \\ 0 \end{Bmatrix}, \quad \bar{\Phi}_6 = \begin{Bmatrix} 0 \\ 0 \\ 0 \\ 0 \\ 0 \\ c_{66} \end{Bmatrix}$$

and normalized to yield

$$N_i = (\bar{\Phi}_i^T \bar{\Phi}_i)^{-1/2}$$

$$\Phi_i = N_i \bar{\Phi}_i$$

In the case of degenerate eigenvalues, the associated eigenvectors are discarded and replaced by vectors orthonormalized to the independent eigenvectors using the standard Gram-Schmidt procedure. In addition, the inverse of the distributing matrix is obtained by simply replacing the diagonal Λ matrix in the above with the following

$$\Lambda^{-1/2} = diag[\varphi_1^{-1/2}, \varphi_2^{-1/2}, \varphi_3^{-1/2}, \varphi_4^{-1/2}, \varphi_5^{-1/2}, \varphi_6^{-1/2}]$$

APPENDIX II

ORTHONORMAL STRESS MODE COEFFICIENTS FOR THE 3-D PIAN-TONG HEXAHEDRAL ELEMENT

For 3-D coordinate transformations, the determinant of the Jacobian is given by

$$\begin{aligned}|\mathbf{J}| \;=\; & s_1 + s_2\xi + s_3\eta + s_4\zeta + s_5\eta\xi + s_6\zeta\xi + s_7\zeta\eta + s_8\xi^2 + s_9\eta^2 + s_{10}\zeta^2 + s_{11}\zeta\eta\xi + s_{12}\eta\xi^2 + \\ & s_{13}\zeta\xi^2 + s_{14}\xi\eta^2 + s_{15}\zeta\eta^2 + s_{16}\xi\zeta^2 + s_{17}\eta\zeta^2 + s_{18}\zeta\eta\xi^2 + s_{19}\zeta\xi\eta^2 + s_{20}\eta\xi\zeta^2\end{aligned}$$

where

$$\begin{array}{llllllllll}
s_1 = \varphi^3_{12} & & s_6 = \varphi^7_{31} + \varphi^6_{51} + \varphi^5_{43} & & s_{11} = 2\varphi^6_{54} & & s_{16} = \varphi^7_{35} \\
s_2 = \varphi^4_{31} + \varphi^5_{12} & & s_7 = \varphi^7_{23} + \varphi^6_{34} + \varphi^5_{26} & & s_{12} = \varphi^7_{14} & & s_{17} = \varphi^6_{37} \\
s_3 = \varphi^4_{23} + \varphi^6_{12} & & s_8 = \varphi^5_{14} & & s_{13} = \varphi^7_{51} & & s_{18} = \varphi^7_{54} \\
s_4 = \varphi^6_{31} + \varphi^5_{23} & & s_9 = \varphi^6_{42} & & s_{14} = \varphi^7_{42} & & s_{19} = \varphi^7_{46} \\
s_5 = \varphi^5_{42} + \varphi^6_{14} + \varphi^7_{12} & & s_{10} = \varphi^6_{35} & & s_{15} = \varphi^7_{26} & & s_{20} = \varphi^7_{65}
\end{array}$$

and

$$\varphi^i_{jk} = a_i(b_jc_k - b_kc_j) + b_i(c_ja_k - c_ka_j) + c_i(a_jb_k - a_kb_j)$$

The stress mode coefficients, r_{ij}, are given by

$$\begin{aligned}
r_{i,1} &= c_{i2} \\
r_{i,2} &= -c_{i2}\lambda_2/\lambda_1 \\
r_{i,3} &= c_{i3} - \phi^1_1 r_{i,1} \\
r_{i,4} &= -c_{i3}\lambda_2/\lambda_1 - \phi^1_1 r_{i,2} \\
r_{i,5} &= c_{i5} - \phi^2_1 r_{i,3} - \phi^2_2 r_{i,1} \\
r_{i,6} &= -\phi^2_1 r_{i,4} - \phi^2_2 r_{i,2} - c_{i5}\lambda_2/\lambda_1 \\
r_{i,7} &= c_{i1} \\
r_{i,8} &= -\phi^3_1 r_{i,5} - \phi^3_2 r_{i,3} - \phi^3_3 r_{i,1} \\
r_{i,9} &= -\phi^3_1 r_{i,6} - \phi^3_2 r_{i,4} - \phi^3_3 r_{i,2} - c_{i1}\lambda_3/\lambda_1 \\
r_{i,10} &= c_{i3} - \phi^4_1 r_{i,7} \\
r_{i,11} &= -\phi^4_1 r_{i,8} - \phi^4_2 r_{i,5} - \phi^4_3 r_{i,3} - \phi^4_4 r_{i,1} \\
r_{i,12} &= -\phi^4_1 r_{i,9} - \phi^4_2 r_{i,6} - \phi^4_3 r_{i,4} - \phi^4_4 / r_{i,2} - c_{i3}\lambda_3/\lambda_1 \\
r_{i,13} &= c_{i6} - \phi^5_1 r_{i,10} - \phi^5_2 r_{i,7} \\
r_{i,14} &= -\phi^5_1 r_{i,11} - \phi^5_2 r_{i,8} - \phi^5_3 r_{i,5} - \phi^5_4 r_{i,3} - \phi^5_5 r_{i,1} \\
r_{i,15} &= -\phi^5_1 r_{i,12} - \phi^5_2 r_{i,9} - \phi^5_3 r_{i,6} - \phi^5_4 r_{i,4} - \phi^5_5 r_{i,2} - \\
&\quad c_{i6}\lambda_3/\lambda_1 \\
r_{i,16} &= c_{i1} \\
r_{i,17} &= -\phi^6_1 r_{i,13} - \phi^6_2 r_{i,10} - \phi^6_3 r_{i,7} \\
r_{i,18} &= -\phi^6_1 r_{i,14} - \phi^6_2 r_{i,11} - \phi^6_3 r_{i,8} - \phi^6_4 r_{i,5} - \phi^6_5 r_{i,3} - \\
&\quad \phi^6_6 r_{i,1} \\
r_{i,19} &= -\phi^6_1 r_{i,15} - \phi^6_2 r_{i,12} - \phi^6_3 r_{i,9} - \phi^6_4 r_{i,6} - \phi^6_5 r_{i,4} - \\
&\quad \phi^6_6 r_{i,2} - c_{i1}\lambda_4/\lambda_1 \\
r_{i,28} &= c_{i3} \\
r_{i,29} &= -\phi^9_1 r_{i,24} - \phi^9_2 r_{i,20} - \phi^9_3 c_{i1} \\
r_{i,30} &= -\phi^9_1 r_{i,25} - \phi^9_2 r_{i,21} - \phi^9_3 r_{i,17} - \phi^9_4 r_{i,13} - \\
&\quad \phi^9_5 r_{i,10} - \phi^9_6 r_{i,7} \\
r_{i,31} &= -\phi^9_1 r_{i,26} - \phi^9_2 r_{i,22} - \phi^9_3 r_{i,18} - \phi^9_4 r_{i,14} - \\
&\quad \phi^9_5 r_{i,11} - \phi^9_6 r_{i,8} - \phi^9_7 r_{i,5} - \phi^9_8 r_{i,3} - \phi^9_9 r_{i,1} \\
r_{i,32} &= -\phi^9_1 r_{i,27} - \phi^9_2 r_{i,23} - \phi^9_3 r_{i,19} - \phi^9_4 r_{i,15} - \\
&\quad \phi^9_5 r_{i,12} - \phi^9_6 r_{i,9} - \phi^9_7 r_{i,6} - \phi^9_8 r_{i,4} - \phi^9_9 r_{i,2} - \\
&\quad c_{i3}\lambda_5/\lambda_1 \\
r_{i,33} &= c_{i1} \\
r_{i,34} &= -\phi^{10}_1 r_{i,28} \\
r_{i,35} &= -\phi^{10}_1 r_{i,29} - \phi^{10}_2 r_{i,24} - \phi^{10}_3 r_{i,20} - \phi^{10}_4 c_{i1} \\
r_{i,36} &= -\phi^{10}_1 r_{i,30} - \phi^{10}_2 r_{i,25} - \phi^{10}_3 r_{i,21} - \phi^{10}_4 r_{i,17} - \\
&\quad \phi^{10}_5 r_{i,13} - \phi^{10}_6 r_{i,10} - \phi^{10}_7 r_{i,7} \\
r_{i,37} &= -\phi^{10}_1 r_{i,31} - \phi^{10}_2 r_{i,26} - \phi^{10}_3 r_{i,22} - \phi^{10}_4 r_{i,18} - \\
&\quad \phi^{10}_5 r_{i,14} - \phi^{10}_6 r_{i,11} - \phi^{10}_7 r_{i,8} - \phi^{10}_8 r_{i,5} - \\
&\quad \phi^{10}_{10} r_{i,1} \\
r_{i,38} &= -\phi^{10}_1 r_{i,32} - \phi^{10}_2 r_{i,27} - \phi^{10}_3 r_{i,23} - \phi^{10}_4 r_{i,19} - \\
&\quad \phi^{10}_5 r_{i,15} - \phi^{10}_6 r_{i,12} - \phi^{10}_7 r_{i,9} - \phi^{10}_8 r_{i,6} - \\
&\quad \phi^{10}_9 r_{i,4} - \phi^{10}_{10} r_{i,2} - c_{i1}\lambda_6/\lambda_1 \\
r_{i,39} &= c_{i2} \\
r_{i,40} &= -\phi^{11}_1 r_{i,33}
\end{aligned}$$

$$
\begin{aligned}
r_{i,20} &\doteq c_{i2} - \phi_1^7 c_{i1} \\
r_{i,21} &= -\phi_1^7 r_{i,17} - \phi_2^7 r_{i,13} - \phi_3^7 r_{i,10} - \phi_4^7 r_{i,7} \\
r_{i,22} &= -\phi_1^7 r_{i,18} - \phi_2^7 r_{i,14} - \phi_3^7 r_{i,11} - \phi_4^7 r_{i,8} - \phi_5^7 r_{i,5} - \\
&\quad \phi_6^7 r_{i,3} - \phi_7^7 r_{i,1} \\
r_{i,23} &= -\phi_1^7 r_{i,19} - \phi_2^7 r_{i,15} - \phi_3^7 r_{i,12} - \phi_4^7 r_{i,9} - \phi_5^7 r_{i,6} - \\
&\quad \phi_6^7 r_{i,4} - \phi_7^7 r_{i,2} - c_{i2}\lambda_4/\lambda_1 \\
r_{i,24} &= c_{i4} - \phi_1^8 r_{i,20} - \phi_2^8 c_{i1} \\
r_{i,25} &= -\phi_1^8 r_{i,21} - \phi_2^8 r_{i,17} - \phi_3^8 r_{i,13} - \phi_4^8 r_{i,10} - \phi_5^8 r_{i,7} \\
r_{i,26} &= -\phi_1^8 r_{i,22} - \phi_2^8 r_{i,18} - \phi_3^8 r_{i,14} - \phi_4^8 r_{i,11} - \phi_5^8 r_{i,8} - \\
&\quad \phi_6^8 r_{i,5} - \phi_7^8 r_{i,3} - \phi_8^8 r_{i,1} \\
r_{i,27} &= -\phi_1^8 r_{i,23} - \phi_2^8 r_{i,19} - \phi_3^8 r_{i,15} - \phi_4^8 r_{i,12} - \phi_5^8 r_{i,9} - \\
&\quad \phi_6^8 r_{i,6} - \phi_7^8 r_{i,4} - \phi_8^8 r_{i,2} - c_{i4}\lambda_4/\lambda_1 \\
r_{i,41} &= -\phi_1^{11} r_{i,34} - \phi_2^{11} r_{i,28} \\
r_{i,42} &= -\phi_1^{11} r_{i,35} - \phi_2^{11} r_{i,29} - \phi_3^{11} r_{i,24} - \phi_4^{11} r_{i,20} - \\
&\quad \phi_5^{11} c_{i1} \\
r_{i,43} &= -\phi_1^{11} r_{i,36} - \phi_2^{11} r_{i,30} - \phi_3^{11} r_{i,25} - \phi_4^{11} r_{i,21} - \\
&\quad \phi_5^{11} r_{i,17} - \phi_6^{11} r_{i,13} - \phi_7^{11} r_{i,10} - \phi_8^{11} r_{i,7} \\
r_{i,44} &= -\phi_1^{11} r_{i,37} - \phi_2^{11} r_{i,31} - \phi_3^{11} r_{i,26} - \phi_4^{11} r_{i,22} - \\
&\quad \phi_5^{11} r_{i,18} - \phi_6^{11} r_{i,14} - \phi_7^{11} r_{i,11} - \phi_8^{11} r_{i,8} - \\
&\quad \phi_9^{11} r_{i,5} - \phi_{10}^{11} r_{i,3} - \phi_{11}^{11} r_{i,1} \\
r_{i,45} &= -\phi_1^{11} r_{i,38} - \phi_2^{11} r_{i,32} - \phi_3^{11} r_{i,27} - \phi_4^{11} r_{i,23} - \\
&\quad \phi_5^{11} r_{i,19} - \phi_6^{11} r_{i,15} - \phi_7^{11} r_{i,12} - \phi_8^{11} r_{i,9} - \\
&\quad \phi_9^{11} r_{i,6} - \phi_{10}^{11} r_{i,4} - \phi_{11}^{11} r_{i,2} - c_{i2}\lambda_7/\lambda_1
\end{aligned}
$$

Expressions for the inner products arising from orthogonalization are given by

$$\phi_n^m = \sum_{i=1}^{6} \phi_{n,i}^m$$

where

$$
\begin{aligned}
\phi_{1,i}^8 &= n_7^2 c_{i,3}(r_{i,1}\lambda_8 + r_{i,2}\lambda_2) \\
\phi_{2,i}^9 &= n_7^2 c_{i,5}(r_{i,1}\lambda_8 + r_{i,2}\lambda_2) \\
\phi_{1,i}^9 &= n_8^2 c_{i,5}(r_{i,3}\lambda_8 + r_{i,4}\lambda_2) \\
\phi_{1,i}^{10} &= n_9^2 c_{i,1}(r_{i,5}\lambda_5 + r_{i,6}\lambda_3) \\
\phi_{3,i}^{10} &= n_7^2 c_{i,1}(r_{i,1}\lambda_5 + r_{i,2}\lambda_3) \\
\phi_{2,i}^{10} &= n_8^2 c_{i,1}(r_{i,3}\lambda_5 + r_{i,4}\lambda_3) \\
\phi_{2,i}^{11} &= n_9^2 c_{i,3}(r_{i,5}\lambda_5 + r_{i,6}\lambda_3) \\
\phi_{3,i}^{11} &= n_8^2 c_{i,3}(r_{i,3}\lambda_5 + r_{i,4}\lambda_3) \\
\phi_{4,i}^{11} &= n_7^2 c_{i,3}(r_{i,1}\lambda_5 + r_{i,2}\lambda_3) \\
\phi_{3,i}^{12} &= n_9^2 c_{i,6}(r_{i,5}\lambda_5 + r_{i,6}\lambda_3) \\
\phi_{4,i}^{12} &= n_8^2 c_{i,6}(r_{i,3}\lambda_5 + r_{i,4}\lambda_3) \\
\phi_{5,i}^{12} &= n_7^2 c_{i,6}(r_{i,1}\lambda_5 + r_{i,2}\lambda_3) \\
\phi_{4,i}^{13} &= n_9^2 c_{i,1}(r_{i,5}\lambda_7 + r_{i,6}\lambda_4) \\
\phi_{5,i}^{13} &= n_8^2 c_{i,1}(r_{i,3}\lambda_7 + r_{i,4}\lambda_4) \\
\phi_{6,i}^{13} &= n_7^2 c_{i,1}(r_{i,1}\lambda_7 + r_{i,2}\lambda_4) \\
\phi_{5,i}^{14} &= n_9^2 c_{i,2}(r_{i,5}\lambda_7 + r_{i,6}\lambda_4) \\
\phi_{6,i}^{14} &= n_8^2 c_{i,2}(r_{i,3}\lambda_7 + r_{i,4}\lambda_4) \\
\phi_{7,i}^{14} &= n_7^2 c_{i,2}(r_{i,1}\lambda_7 + r_{i,2}\lambda_4) \\
\phi_{6,i}^{15} &= n_9^2 c_{i,4}(r_{i,5}\lambda_7 + r_{i,6}\lambda_4) \\
\phi_{7,i}^{15} &= n_8^2 c_{i,4}(r_{i,3}\lambda_7 + r_{i,4}\lambda_4) \\
\phi_{8,i}^{15} &= n_7^2 c_{i,4}(r_{i,1}\lambda_7 + r_{i,2}\lambda_4) \\
\phi_{7,i}^{16} &= n_9^2 c_{i,3}(r_{i,5}\lambda_{14} + r_{i,6}\lambda_5) \\
\phi_{8,i}^{16} &= n_8^2 c_{i,3}(r_{i,3}\lambda_{14} + r_{i,4}\lambda_5) \\
\phi_{9,i}^{16} &= n_7^2 c_{i,3}(r_{i,1}\lambda_{14} + r_{i,2}\lambda_5) \\
\phi_{8,i}^{17} &= n_9^2 c_{i,1}(r_{i,5}\lambda_{11} + r_{i,6}\lambda_6) \\
\phi_{9,i}^{17} &= n_8^2 c_{i,1}(r_{i,3}\lambda_{11} + r_{i,4}\lambda_6) \\
\phi_{10,i}^{17} &= n_7^2 c_{i,1}(r_{i,1}\lambda_{11} + r_{i,2}\lambda_6) \\
\phi_{9,i}^{18} &= n_9^2 c_{i,2}(r_{i,5}\lambda_{16} + r_{i,6}\lambda_7) \\
\phi_{10,i}^{18} &= n_8^2 c_{i,2}(r_{i,3}\lambda_{16} + r_{i,4}\lambda_7) \\
\phi_{11,i}^{18} &= n_7^2 c_{i,2}(r_{i,1}\lambda_{16} + r_{i,2}\lambda_7) \\
\phi_{1,i}^{11} &= n_{10}^2 c_{i,3}(r_{i,7}\lambda_9 + r_{i,8}\lambda_5 + r_{i,9}\lambda_3) \\
\phi_{1,i}^{12} &= n_{11}^2 c_{i,6}(r_{i,10}\lambda_9 + r_{i,11}\lambda_5 + r_{i,12}\lambda_3) \\
\phi_{2,i}^{12} &= n_{10}^2 c_{i,6}(r_{i,7}\lambda_9 + r_{i,8}\lambda_5 + r_{i,9}\lambda_3) \\
\phi_{1,i}^{13} &= n_{12}^2 c_{i,1}(r_{i,13}\lambda_6 + r_{i,14}\lambda_7 + r_{i,15}\lambda_4) \\
\phi_{2,i}^{13} &= n_{11}^2 c_{i,1}(r_{i,10}\lambda_6 + r_{i,11}\lambda_7 + r_{i,12}\lambda_4) \\
\phi_{3,i}^{13} &= n_{10}^2 c_{i,1}(r_{i,7}\lambda_6 + r_{i,8}\lambda_7 + r_{i,9}\lambda_4) \\
\phi_{2,i}^{14} &= n_{12}^2 c_{i,2}(r_{i,13}\lambda_6 + r_{i,14}\lambda_7 + r_{i,15}\lambda_4) \\
\phi_{3,i}^{14} &= n_{11}^2 c_{i,2}(r_{i,10}\lambda_6 + r_{i,11}\lambda_7 + r_{i,12}\lambda_4) \\
\phi_{4,i}^{14} &= n_{10}^2 c_{i,2}(r_{i,7}\lambda_6 + r_{i,8}\lambda_7 + r_{i,9}\lambda_4) \\
\phi_{3,i}^{15} &= n_{12}^2 c_{i,4}(r_{i,13}\lambda_6 + r_{i,14}\lambda_7 + r_{i,15}\lambda_4) \\
\phi_{4,i}^{15} &= n_{11}^2 c_{i,4}(r_{i,10}\lambda_6 + r_{i,11}\lambda_7 + r_{i,12}\lambda_4) \\
\phi_{5,i}^{15} &= n_{10}^2 c_{i,4}(r_{i,7}\lambda_6 + r_{i,8}\lambda_7 + r_{i,9}\lambda_4) \\
\phi_{4,i}^{16} &= n_{12}^2 c_{i,3}(r_{i,13}\lambda_{12} + r_{i,14}\lambda_{14} + r_{i,15}\lambda_5) \\
\phi_{5,i}^{16} &= n_{11}^2 c_{i,3}(r_{i,10}\lambda_{12} + r_{i,11}\lambda_{14} + r_{i,12}\lambda_5) \\
\phi_{6,i}^{16} &= n_{10}^2 c_{i,3}(r_{i,7}\lambda_{12} + r_{i,8}\lambda_{14} + r_{i,9}\lambda_5) \\
\phi_{5,i}^{17} &= n_{12}^2 c_{i,1}(r_{i,13}\lambda_{17} + r_{i,14}\lambda_{11} + r_{i,15}\lambda_6) \\
\phi_{6,i}^{17} &= n_{11}^2 c_{i,1}(r_{i,10}\lambda_{17} + r_{i,11}\lambda_{11} + r_{i,12}\lambda_6) \\
\phi_{7,i}^{17} &= n_{10}^2 c_{i,1}(r_{i,7}\lambda_{17} + r_{i,8}\lambda_{11} + r_{i,9}\lambda_6) \\
\phi_{6,i}^{18} &= n_{12}^2 c_{i,2}(r_{i,13}\lambda_{11} + r_{i,14}\lambda_{16} + r_{i,15}\lambda_7) \\
\phi_{7,i}^{18} &= n_{11}^2 c_{i,2}(r_{i,10}\lambda_{11} + r_{i,11}\lambda_{16} + r_{i,12}\lambda_7) \\
\phi_{8,i}^{18} &= n_{10}^2 c_{i,2}(r_{i,7}\lambda_{11} + r_{i,8}\lambda_{16} + r_{i,9}\lambda_7) \\
\phi_{1,i}^{14} &= n_{13}^2 c_{i,2}(r_{i,16}\lambda_{10} + r_{i,17}\lambda_6 + r_{i,18}\lambda_7 + r_{i,19}\lambda_4) \\
\phi_{1,i}^{15} &= n_{14}^2 c_{i,4}(r_{i,20}\lambda_{10} + r_{i,21}\lambda_6 + r_{i,22}\lambda_7 + r_{i,23}\lambda_4) \\
\phi_{2,i}^{15} &= n_{13}^2 c_{i,4}(r_{i,16}\lambda_{10} + r_{i,17}\lambda_6 + r_{i,18}\lambda_7 + r_{i,19}\lambda_4) \\
\phi_{1,i}^{16} &= n_{15}^2 c_{i,3}(r_{i,24}\lambda_{11} + r_{i,25}\lambda_{12} + r_{i,26}\lambda_{14} + r_{i,27}\lambda_5) \\
\phi_{2,i}^{16} &= n_{14}^2 c_{i,3}(r_{i,20}\lambda_{11} + r_{i,21}\lambda_{12} + r_{i,22}\lambda_{14} + r_{i,23}\lambda_5) \\
\phi_{3,i}^{16} &= n_{13}^2 c_{i,3}(r_{i,16}\lambda_{11} + r_{i,17}\lambda_{12} + r_{i,18}\lambda_{14} + r_{i,19}\lambda_5) \\
\phi_{2,i}^{17} &= n_{15}^2 c_{i,1}(r_{i,24}\lambda_{15} + r_{i,25}\lambda_{17} + r_{i,26}\lambda_{11} + r_{i,27}\lambda_6) \\
\phi_{3,i}^{17} &= n_{14}^2 c_{i,1}(r_{i,20}\lambda_{15} + r_{i,21}\lambda_{17} + r_{i,22}\lambda_{11} + r_{i,23}\lambda_6) \\
\phi_{4,i}^{17} &= n_{13}^2 c_{i,1}(r_{i,16}\lambda_{15} + r_{i,17}\lambda_{17} + r_{i,18}\lambda_{11} + r_{i,19}\lambda_6) \\
\phi_{3,i}^{18} &= n_{15}^2 c_{i,2}(r_{i,24}\lambda_{13} + r_{i,25}\lambda_{11} + r_{i,26}\lambda_{16} + r_{i,27}\lambda_7) \\
\phi_{4,i}^{18} &= n_{14}^2 c_{i,2}(r_{i,20}\lambda_{13} + r_{i,21}\lambda_{11} + r_{i,22}\lambda_{16} + r_{i,23}\lambda_7) \\
\phi_{5,i}^{18} &= n_{13}^2 c_{i,2}(r_{i,16}\lambda_{13} + r_{i,17}\lambda_{11} + r_{i,18}\lambda_{16} + r_{i,19}\lambda_7) \\
\phi_{1,i}^{17} &= n_{16}^2 c_{i,1}(r_{i,28}\lambda_{22} + r_{i,29}\lambda_{15} + r_{i,30}\lambda_{17} + r_{i,31}\lambda_{11} + \\
&\quad r_{i,32}\lambda_6) \\
\phi_{2,i}^{18} &= n_{16}^2 c_{i,2}(r_{i,28}\lambda_{23} + r_{i,29}\lambda_{13} + r_{i,30}\lambda_{11} + r_{i,31}\lambda_{16} + \\
&\quad r_{i,32}\lambda_7) \\
\phi_{1,i}^{18} &= n_{17}^2 c_{i,2}(r_{i,33}\lambda_{21} + r_{i,34}\lambda_{23} + r_{i,35}\lambda_{13} + r_{i,36}\lambda_{11} + \\
&\quad r_{i,37}\lambda_{16} + r_{i,38}\lambda_7)
\end{aligned}
$$

Normalizing factors for the othogonal stress modes in which $j = 1, 2, 3$ are given by

$$
\begin{aligned}
n_1 &= \lambda_1^{-1/2} \\
n_{j+6} &= \{\textstyle\sum_{i=1}^{6}(r_{i,2j-1}^2\lambda_8 + r_{i,2j-1}r_{i,2j}\lambda_2 + r_{i,2j}^2\lambda_1)\}^{-1/2} \\
n_{j+9} &= \{\textstyle\sum_{i=1}^{6}(r_{i,3j+4}^2\lambda_9 + 2r_{i,3j+4}(r_{i,3j+5}\lambda_5 + r_{i,3j+6}\lambda_3) + r_{i,3j+5}^2\lambda_8 + 2r_{i,3j+5}r_{i,3j+6}\lambda_2 + \\
&\quad r_{i,3j+6}^2\lambda_1)\}^{-1/2} \\
n_{j+12} &= \{\textstyle\sum_{i=1}^{6}(r_{i,4j+12}^2\lambda_{10} + 2r_{i,4j+12}(r_{i,4j+13}\lambda_6 + r_{i,4j+14}\lambda_7 + r_{i,4j+15}\lambda_4) + r_{i,4j+13}^2\lambda_9 + \\
&\quad 2r_{i,4j+13}(r_{i,4j+14}\lambda_5 + r_{i,4j+15}\lambda_3) + r_{i,4j+14}^2\lambda_8 + 2r_{i,4j+14}r_{i,4j+15}\lambda_2 + r_{i,4j+15}^2\lambda_1)\}^{-1/2} \\
n_{16} &= \{\textstyle\sum_{i=1}^{6}(r_{i,28}^2\lambda_{18} + 2r_{i,28}(r_{i,29}\lambda_{11} + r_{i,30}\lambda_{12} + r_{i,31}\lambda_{14} + r_{i,32}\lambda_5) + r_{i,29}^2\lambda_{10} + \\
&\quad 2r_{i,29}(r_{i,30}\lambda_6 + r_{i,31}\lambda_7 + r_{i,32}\lambda_4) + r_{i,30}^2\lambda_9 + 2r_{i,30}(r_{i,31}\lambda_5 + \\
&\quad r_{i,32}\lambda_3) + r_{i,31}^2\lambda_8 + 2r_{i,31}r_{i,32}\lambda_2 + r_{i,32}^2\lambda_1)\}^{-1/2} \\
n_{17} &= \{\textstyle\sum_{i=1}^{6}(r_{i,33}^2\lambda_{19} + 2r_{i,33}(r_{i,34}\lambda_{22} + r_{i,35}\lambda_{15} + r_{i,36}\lambda_{17} + r_{i,37}\lambda_{11} + r_{i,38}\lambda_6) + \\
&\quad r_{i,34}^2\lambda_{18} + 2r_{i,34}(r_{i,35}\lambda_{11} + r_{i,36}\lambda_{12} + r_{i,37}\lambda_{14} + r_{i,38}\lambda_5) + r_{i,35}^2\lambda_{10} + \\
&\quad 2r_{i,35}(r_{i,36}\lambda_6 + r_{i,37}\lambda_7 + r_{i,38}\lambda_4) + r_{i,36}^2\lambda_9 + 2r_{i,36}(r_{i,37}\lambda_5 + r_{i,38}\lambda_3) + \\
&\quad r_{i,37}^2\lambda_8 + 2r_{i,37}r_{i,38}\lambda_2 + r_{i,38}^2\lambda_1)\}^{-1/2} \\
n_{18} &= \{\textstyle\sum_{i=1}^{6}(r_{i,39}^2\lambda_{20} + 2r_{i,39}(r_{i,40}\lambda_{21} + r_{i,41}\lambda_{23} + r_{i,42}\lambda_{13} + r_{i,43}\lambda_{11} + r_{i,44}\lambda_{16} + r_{i,45}\lambda_7) + \\
&\quad r_{i,40}^2\lambda_{19} + 2r_{i,40}(r_{i,41}\lambda_{22} + r_{i,42}\lambda_{15} + r_{i,43}\lambda_{17} + r_{i,44}\lambda_{11} + r_{i,45}\lambda_6) + r_{i,41}^2\lambda_{18} + \\
&\quad 2r_{i,41}(r_{i,42}\lambda_{11} + r_{i,43}\lambda_{12} + r_{i,44}\lambda_{14} + r_{i,45}\lambda_5) + r_{i,42}^2\lambda_{10} + 2r_{i,42}(r_{i,43}\lambda_6 + \\
&\quad r_{i,44}\lambda_7 + r_{i,45}\lambda_4) + r_{i,43}^2\lambda_9 + 2r_{i,43}(r_{i,44}\lambda_5 + r_{i,45}\lambda_3 + \\
&\quad r_{i,44}^2\lambda_8 + 2r_{i,44}r_{i,45}\lambda_2 + r_{i,45}^2\lambda_1)\}^{-1/2}
\end{aligned}
$$

The integrals arising in the weighted inner product evaluate to

$$
\begin{aligned}
\lambda_1 &= 8(3s_1 + s_8 + s_9 + s_{10})/3 \\
\lambda_2 &= 8(3s_2 + s_{14} + s_{16})/9 \\
\lambda_3 &= 8(3s_3 + s_{12} + s_{17})/9 \\
\lambda_4 &= 8(3s_4 + s_{13} + s_{15})/9 \\
\lambda_5 &= 8(3s_5 + s_{20})/27 \\
\lambda_6 &= 8(3s_7 + s_{18})/27 \\
\lambda_7 &= 8(3s_6 + s_{19})/27 \\
\lambda_8 &= 8(15s_1 + 9s_8 + 5s_9 + 5s_{10})/45 \\
\lambda_9 &= 8(15s_1 + 5s_8 + 9s_9 + 5s_{10})/45 \\
\lambda_{10} &= 8(15s_1 + 5s_8 + 5s_9 + 9s_{10})/45 \\
\lambda_{11} &= 8s_{11}/27 \\
\lambda_{12} &= 8(15s_2 + 9s_{14} + 5s_{16})/135 \\
\lambda_{13} &= 8(15s_2 + 5s_{14} + 9s_{16})/135 \\
\lambda_{14} &= 8(15s_3 + 9s_{12} + 5s_{17})/135 \\
\lambda_{15} &= 8(15s_3 + 5s_{12} + 9s_{17})/135 \\
\lambda_{16} &= 8(15s_4 + 9s_{13} + 5s_{15})/135 \\
\lambda_{17} &= 8(15s_4 + 5s_{13} + 9s_{15})/135 \\
\lambda_{18} &= 8(15s_1 + 9s_8 + 9s_9 + 5s_{10})/135 \\
\lambda_{19} &= 8(15s_1 + 5s_8 + 9s_9 + 9s_{10})/135 \\
\lambda_{20} &= 8(15s_1 + 9s_8 + 5s_9 + 9s_{10})/135 \\
\lambda_{21} &= 8(5s_5 + 3s_{20})/135 \\
\lambda_{22} &= 8(5s_6 + 3s_{19})/135 \\
\lambda_{23} &= 8(5s_7 + 3s_{18})/135
\end{aligned}
$$

APPENDIX III

ORTHONORMAL STRESS MODE COEFICIENTS FOR THE NONLINEAR PIAN-SUMIHARA ELEMENT

The stress mode coefficients, p_{ij}^*, are given by

$$
\begin{array}{llllll}
p_{13}^* = n_1 & p_{42}^* = n_4c_{11} & p_{43}^* = -n_4c_{11}\lambda_2/\lambda_1 \\
p_{26}^* = n_1 & p_{45}^* = n_4c_{21} & p_{46}^* = -n_4c_{21}\lambda_2/\lambda_1 \\
p_{39}^* = n_1 & p_{48}^* = n_4c_{31} & p_{49}^* = -n_4c_{31}\lambda_2/\lambda_1 \\
p_{51}^* = n_5c_{12} & p_{52}^* = -n_5c_{11}\phi & p_{53}^* = -n_5\theta_1 \\
p_{54}^* = n_5c_{22} & p_{55}^* = -n_5c_{21}\phi & p_{56}^* = -n_5\theta_2 \\
p_{57}^* = n_5c_{32} & p_{58}^* = -n_5c_{31}\phi & p_{59}^* = -n_5\theta_3
\end{array}
$$

in which

$$
\begin{aligned}
\phi &= -n_4^2(c_{12}c_{11} + c_{22}c_{21} + c_{32}c_{31})\lambda_2\lambda_3/\lambda_1 \\
\theta_1 &= (c_{12}\lambda_3 + \phi c_{11}\lambda_2)/\lambda_1 \\
\theta_2 &= (c_{22}\lambda_3 + \phi c_{21}\lambda_2)/\lambda_1 \\
\theta_3 &= (c_{32}\lambda_3 + \phi c_{31}\lambda_2)/\lambda_1
\end{aligned}
$$

and normalizing factors are given by

$$\begin{aligned} n_1 &= {\lambda_1}^{-1/2} \\ n_4 &= [(c_{11}^2 + c_{21}^2 + c_{31}^2)(\lambda_5 - {\lambda_2}^2/\lambda_1)]^{-1/2} \\ n_5 &= [\sum_{i=1}^{3}(c_{i2}^2 - 2c_{i2}\theta_i\lambda_3 + \phi^2 c_{i1}^2\lambda_5 + 2\phi c_{i1}\theta_i\lambda_2 + \theta_i^2\lambda_1)]^{-1/2} \end{aligned}$$

The determinant of the Jacobian for 2-D transformations is given by

$$|\mathbf{J}| = J_0 + J_1\xi + J_2\eta$$

where

$$J_0 = a_1b_2 - a_2b_1 \quad ; \quad J_1 = a_1b_3 - a_3b_1 \quad ; \quad J_2 = a_3b_2 - a_2b_3$$

The scalar integrals arising in the inner product to evaluate to

$$\lambda_1 = \int_{-1}^{1}\int_{-1}^{1} |\mathbf{J}| d\xi d\eta = 4J_0 \qquad \lambda_4 = \int_{-1}^{1}\int_{-1}^{1} [|\mathbf{J}|\xi\eta d\xi d\eta = 0$$

$$\lambda_2 = \int_{-1}^{1}\int_{-1}^{1} |\mathbf{J}|\xi d\xi d\eta = 4J_1/3 \qquad \lambda_5 = \int_{-1}^{1}\int_{-1}^{1} [|\mathbf{J}|\xi^2 d\xi d\eta = 4J_0/3$$

REFERENCES

1. K. Y. Sze and C. L. Chow, 'Efficient hybrid/mixed elements using admissible matrix formulation', *Comp. Meth. Applied Mech. and Engrg.*, **99**, 1-26 (1992).

2. K. Y. Sze, 'Efficient formulation of robust hybrid elements using orthogonal stress/strain interpolants and admissible matrix formulation', *Int. J. Num. Meth. Engrg.*, **35**, 1-20, (1992).

3. K. Y. Sze, 'A novel approach for devising higher-order hybrid elements,' *Int. J. Num. Meth. Engrg.*, **36**, pp. 3303-3316, (1993).

4. E. Saether, 'Explicit determination of element stiffness matrices in the hybrid stress method,' *Int. J. Num. Meth. Engrg.*, (to appear).

5. T. H. H. Pian and P. Tong, 'Relations between incompatible displacement model and hybrid stress model,' *Int. J. Num. Meth. Engrg.*, **22**, 173-181, (1986).

6. T. H. H. Pian and K. Sumihara, 'Rational approach for assumed stress finite element', *Int. J. Num. Meth. Engrg.*, **20**, 1685-1695, (1984).

7. C. Lanczos, *Applied Analysis,* Dover Publications, (1988).

8. C. C. Wu, M. G. Huang and T. H. H. Pian, 'Consistency condition and convergence criteria of incompatible elements: General formulation of incompatible functions and its application', *Comp. Struct.*, **27**, 639-644, (1988).

DISTRIBUTION LIST

No. of Copies	To
1	Office of the Under Secretary of Defense for Research and Engineering, The Pentagon, Washington, DC 20301
	Director, U.S. Army Research Laboratory, 2800 Powder Mill Road, Adelphi, MD 20783-1197
1	ATTN: AMSRL-OP-SD-TP, Technical Publishing Branch
1	AMSRL-OP-SD-TA, Records Management
1	AMSRL-OP-SD-TL, Technical Library
	Commander, Defense Technical Information Center, Cameron Station, Building 5, 5010 Duke Street, Alexandria, VA 23304-6145
2	ATTN: DTIC-FDAC
1	MIA/CINDAS, Purdue University, 2595 Yeager Road, West Lafayette, IN 47905
	Commander, Army Research Office, P.O. Box 12211, Research Triangle Park, NC 27709-2211
1	ATTN: Information Processing Office
	Commander, U.S. Army Materiel Command, 5001 Eisenhower Avenue, Alexandria, VA 22333
1	ATTN: AMCSCI
1	AMCMI-IS-A
	Commander, U.S. Army Materiel Systems Analysis Activity, Aberdeen Proving Ground, MD 21005
1	ATTN: AMXSY-MP, H. Cohen
	Commander, U.S. Army Missile Command, Redstone Arsenal, AL 35809
1	ATTN: AMSMI-RD-CS-R/Doc
	Commander, U.S. Army - ARDEC, Information Research Center, Picatinny Arsenal, NJ 07806-5000
1	ATTN: AMSTA-AR-IMC, Bldg. 59
	Commander, U.S. Army Natick Research, Development and Engineering Center Natick, MA 01760-5010
1	ATTN: SATNC-MI, Technical Library
1	SATNC-AI
	Commander, U.S. Army Satellite Communications Agency, Fort Monmouth, NJ 07703
1	ATTN: Technical Document Center
	Commander, U.S. Army Tank-Automotive Command, Warren, MI 48397-5000
1	ATTN: AMSTA-ZSK
1	AMSTA-TSL, Technical Library
1	AMSTA-SF
	President, Airborne, Electronics and Special Warfare Board, Fort Bragg, NC 28307
1	ATTN: Library

No. of Copies	To
	Director, U.S. Army Research Laboratory, Weapons Technology, Aberdeen Proving Ground, MD 21005-5066
1	ATTN: AMSRL-WT
2	Technical Library
	Commander, Dugway Proving Ground, UT 84022
1	ATTN: Technical Library, Technical Information Division
	Commander, U.S. Army Research Laboratory, 2800 Powder Mill Road, Adelphi, MD 20783
1	ATTN: AMSRL-SS
	Director, Benet Weapons Laboratory, LCWSL, USA AMCCOM, Watervliet, NY 12189
1	ATTN: AMSMC-LCB-TL
1	AMSMC-LCB-R
1	AMSMC-LCB-RM
1	AMSMC-LCB-RP
	Commander, U.S. Army Foreign Science and Technology Center, 220 7th Street, N.E., Charlottesville, VA 22901-5396
3	ATTN: AIFRTC, Applied Technologies Branch, Gerald Schlesinger
	Commander, U.S. Army Aeromedical Research Unit, P.O. Box 577, Fort Rucker, AL 36360
1	ATTN: Technical Library
	U.S. Army Aviation Training Library, Fort Rucker, AL 36360
1	ATTN: Building 5906-5907
	Commander, U.S. Army Agency for Aviation Safety, Fort Rucker, AL 3636
1	ATTN: Technical Library
	Commander, Clarke Engineer School Library, 3202 Nebraska Ave., N., Fort Leonard Wood, MO 65473-5000
1	ATTN: Library
	Commander, U.S. Army Engineer Waterways Experiment Station, P.O. Box 631, Vicksburg, MS 39180
1	ATTN: Research Center Library
	Commandant, U.S. Army Quartermaster School, Fort Lee, VA 23801
1	ATTN: Quartermaster School Library
	Naval Research Laboratory, Washington, DC 20375
1	ATTN: Code 6384
	Chief of Naval Research, Arlington, VA 22217
1	ATTN: Code 471
	Commander, U.S. Air Force Wright Research and Development Center, Wright-Patterson Air Force Base, OH 45433-6523
1	ATTN: WRDC/MLLP, M. Forney, Jr.
1	WRDC/MLBC, Mr. Stanley Schulman

No. of Copies	To
	U.S. Department of Commerce, National Institute of Standards and Technology, Gaithersburg, MD 20899
1	ATTN: Stephen M. Hsu, Chief, Ceramics Division, Institute for Materials Science and Engineering
1	Committee on Marine Structures, Marine Board, National Research Council, 2101 Constitution Avenue, N.W., Washington, DC 20418
1	Materials Sciences Corporation, Suite 250, 500 Office Center Drive, Fort Washington, PA 19034
1	Charles Stark Draper Laboratory, 555 Technology Square, Cambridge, MA 02139
	General Dynamics, Convair Aerospace Division, P.O. Box 748, Fort Worth, TX 76101
1	ATTN: Mfg. Engineering Technical Library
	Plastics Technical Evaluation Center, PLASTEC, ARDEC, Bldg. 355N, Picatinny Arsenal, NJ 07806-5000
1	ATTN: Harry Pebly
1	Department of the Army, Aerostructures Directorate, MS-266, U.S. Army Aviation R&T Activity - AVSCOM, Langley Research Center, Hampton, VA 23665-5225
1	NASA - Langley Research Center, Hampton, VA 23665-5255
	U.S. Army Vehicle Propulsion Directorate, NASA Lewis Research Center, 2100 Brookpark Road, Cleveland, OH 44135-3191
1	ATTN: AMSRL-VP
	Director, Defense Intelligence Agency, Washington, DC 20340-6053
1	ATTN: ODT-5A, Mr. Frank Jaeger
	U.S. Army Communications and Electronics Command, Fort Monmouth, NJ 07703
1	ATTN: Technical Library
	U.S. Army Research Laboratory, Electronic Power Sources Directorate, Fort Monmouth, NJ 07703
1	ATTN: Technical Library
	Director, U.S. Army Research Laboratory, Watertown, MA 02172-0001
2	ATTN: AMSRL-OP-WT-IS, Technical Library
5	Author